Animal Nutrition 19 (2024) 192–214

Contents lists available at ScienceDirect

Animal Nutrition

journal homepage: http://www.keaipublishing.com/en/journals/aninu/

Original Research Article

Effects of aflatoxin B1 on subacute exposure of hybrid groupers (*Epinephelus fuscoguttatus*♀ × *Epinephelus lanceolatus*♂): Growth, liver histology, and integrated liver transcriptome and metabolome analysis

Hao Liu [a, b], Shuqing Liang [a, b], Weibin Huang [a, b], Yuanzhi Yang [a, b], Menglong Zhou [a, b], Baiquan Lu [a, b], Biao Li [a, b], Wenshan Cai [a, b], Hengyang Song [a, b], Beiping Tan [a, b, c, *], Xiaohui Dong [a, b, c, *]

[a] *Laboratory of Aquatic Animal Nutrition and Feed, College of Fisheries, Guangdong Ocean University, Zhanjiang 524088, China*
[b] *Aquatic Animals Precision Nutrition and High-Efficiency Feed Engineering Research Centre of Guangdong Province, Zhanjiang 524088, China*
[c] *Key Laboratory of Aquatic, Livestock and Poultry Feed Science and Technology in South China, Ministry of Agriculture and Rural Affairs, Zhanjiang 524000, China*

ARTICLE INFO

Article history:
Received 18 February 2024
Received in revised form
27 July 2024
Accepted 9 August 2024
Available online 31 August 2024

Keywords:
Aflatoxin B1
Hybrid grouper
Transcriptomic
Metabolomic
Liver

ABSTRACT

With the increasing incorporation of plant-based ingredients into the grouper diet, the issue of aflatoxin B1 (AFB1) contamination in the diet has become a significant concern. In this study, the negative effects of AFB1 on the growth and liver health of hybrid groupers (*Epinephelus fuscoguttatus*♀ × *Epinephelus lanceolatus*♂) were investigated in the context of growth, liver histology, serum biochemical indices, and integrated transcriptomic and metabolomic data. A total of 540 healthy hybrid groupers, initially weighing 11.59 ± 0.03 g, were randomly divided into six groups (three replicates of 30 fish each): the control group was fed a basal diet, and the experimental groups were supplemented with 7 (AF7), 30 (AF30), 111 (AF111), 445 (AF445) and 2230 μg/kg AFB1 (AF2230) in the basal diet respectively, for 56 days. Groups control, AF445, and AF2230 were selected for subsequent histological, muscle fatty acid, and transcriptomic and metabolomic analyses based on the results of hybrid grouper growth and serum biochemical indices. Compared to the control group, both whole-body crude lipid and muscle crude lipid contents showed significant decreases in the AF2230 group ($P < 0.05$), while only muscle crude lipid content showed a significant decrease in the AF445 group ($P = 0.001$). Liver damage was seen in the histology of the liver of AF445 and AF2230 groups. Muscle fatty acid results showed that the addition of 445 and 2230 μg/kg AFB1 to the diets increased saturated fatty acids and monounsaturated fatty acids and decreased polyunsaturated fatty acids and highly unsaturated fatty acids in muscle ($P < 0.05$). Transcriptome analyses revealed multiple metabolic pathways associated with AFB1 metabolism, and metabolomics analyses further confirmed changes in the activity of these pathways. The results of the combined transcriptomic and metabolomic analyses indicated that AFB1 causes liver injury mainly by affecting liver retinol metabolism, metabolism of xenobiotics by cytochromes P450, drug metabolism-cytochromes P450 and biosynthesis of unsaturated fatty acids. In conclusion, dietary AFB1 levels above 445 μg/kg resulted in growth inhibition, liver injury, liver AFB1 accumulation, and reduced muscle polyunsaturated fatty acid content in groupers, thereby affecting muscle quality. This study provides

* Corresponding authors.
E-mail addresses: tanbp@gdou.edu.cn (B. Tan), dongxh@gdou.edu.cn (X. Dong).
Peer review under the responsibility of Chinese Association of Animal Science and Veterinary Medicine.

Production and Hosting by Elsevier on behalf of KeAi

https://doi.org/10.1016/j.aninu.2024.08.002

novel insights into the detrimental effects of AFB1 on aquatic species and contributes to the scientific basis for the health and sustainability of aquaculture practices.

1. Introduction

Aflatoxin B1 (AFB1) contamination of feedstuffs (including grains and oil-rich crops) and foodstuffs such as meat, milk, and eggs poses a broad spectrum of health risks and diseases in humans and cattle (Pauletto et al., 2020; Saba and Seal, 2022). AFB1 is the most potent aflatoxin, demonstrating hepatotoxic, immunotoxic, mutagenic, carcinogenic, and teratogenic characteristics. Compelling evidence indicates that AFB1 is linked to the formation of hepatocellular carcinoma (HCC), leading the International Agency for Research on Cancer (IARC) to classify it as a Group 1 human carcinogen (Zuckerman, 1995). Notably, several studies have underscored the potent synergistic effects of AFB1 exposure and chronic hepatitis C virus infection in humans (Wu et al., 2009).

AFB1 also poses a significant threat to aquatic species in aquaculture, potentially causing growth inhibition, liver damage, and tissue discoloration including the gills, liver, kidneys, spleen, stomach, and intestines (El-Sayed and Khalil, 2009; Farabi et al., 2006; Zychowski et al., 2013). Therefore, exposure of aquatic animals to a diet contaminated with AFB1 can result in substantial financial damages. The sensitivity of fish to aflatoxins varies by species and growth stage, with juveniles and certain species showing higher sensitivity (Royes and Yanong, 2010). Rainbow trout (*Oncorhynchus mykiss*), for instance, are particularly sensitive to AFB1. Exposing rainbow trout to AFB1 at levels as low as 0.4 μg/kg diet for a prolonged period of time has been demonstrated to elevate the likelihood of cancer, as indicated by studies conducted by Mwihia et al. (2018) and Royes and Yanong (2010). When these fish were given a diet with 20 μg/kg AFB1 for periods of 8 and 12 months, the occurrence of liver tumors was 58.0% and 83.0%, respectively (Royes and Yanong, 2010). In addition to cancer, in vitro exposure to AFB1 can cause immunosuppression in rainbow trout (Ottinger and Kaattari, 1998). Experiments have shown that AFB1 has a lethal dose 50% (LD50) of 0.81 mg/kg body weight for rainbow trout, and perch (*Dicentrarchus labrax* L.) and red drum (*Sciaenops ocellatus*) exhibit more sensitivity compared to rainbow trout, with 96-h LD50 of 0.18 mg/kg body weight (El-Sayed and Khalil, 2009) and 0.1 mg/kg body weight (Zychowski et al., 2013), respectively.

In all animal species, AFB1 undergoes bioactivation in the liver by cytochrome P450 enzymes (Rushing and Selim, 2019); in particular, the cytochrome P450 family 1 subfamily A1 (cyp1a) and cytochrome P450 family 3 subfamily A (cyp3a) isoforms produce different toxic metabolites, including AFB1-exo-8, 9-epoxide (AFBO), aflatoxin M1 (AFM1), aflatoxin (AFL), aflatoxin B2a (AFB2a), aflatoxin Q1 (AFQ1), and aflatoxin P1 (AFP1) (Dohnal et al., 2014). The epoxide derivative is the most toxic metabolite of AFB1, potentially binding to guanine residues of nucleic acids (Ghadiri et al., 2019). These adducts can induce DNA mutations, inhibiting DNA transcription and RNA translation (Kuilman et al., 1998; Wogan et al., 2012). AFBO can also be partially hydrolyzed to AFB1-diol either spontaneously or by an epoxide hydrolase (EPHX)-catalyzed reaction. However, this metabolite can bind lysine residues, leading to protein damage and necrosis, thus representing another mechanism of AFB1 toxicity (Kuilman et al., 2000; McLean and Dutton, 1995). The primary detoxification pathway for AFBO involves binding to glutathione, catalyzed by the glutathione S-transferase alpha 1 (gsta1) isoform of glutathione-S-transferase (gst). This reaction converts reactive metabolites into polar and less toxic derivatives that are excreted in the urine (Rushing and Selim, 2019). UDP-glucuronosyltransferases (ugt), crucial in phase II metabolic processes, represent an important class of drug-metabolizing enzymes (Yokoyama et al., 2018), and ugt can participate in the metabolism of AFB1, contributing to its elimination from the body by catalyzing its conjugation with glucuronide to form more polar metabolites (Deng et al., 2020). However, AFB1 has also been shown to affect ugt activity. One study found that AFB1 and its metabolite aflatoxin G1 (AFG1) were able to significantly inhibit certain ugt isoforms, particularly UDP glucuronosyltransferase family 1 member A7 (ugt1a7) and UDP glucuronosyltransferase family 1 member A8 (ugt1a8) (Du and Liu, 2023). Although the role of gst and ugt in AFB1 detoxification has been studied in human cells (Hanioka et al., 2012) and terrestrial animals (Nayak and Sashidhar, 2010), studies involving the expression levels of these enzymes in AFB1-exposed aquatic animals are limited.

Transcriptome sequencing, valued for its high throughput, low cost, and high sensitivity, is extensively utilized in the mechanistic toxicology of mycotoxins (Eshelli et al., 2018). Metabolomics, through the analysis of small tissue samples, allows for the comparison of metabolite alterations across different treatment groups, reflecting the pattern of endogenous metabolite changes throughout the body (Zhang et al., 2022). Metabolomics has recently been widely used in several disciplines such as clinical diagnostics, toxicology, and nutrition (Suzuki, 2005; C. Wang et al., 2021; Xu et al., 2022). Therefore, integrating transcriptome sequencing with metabolomics is essential for understanding the hepatotoxic effects of AFB1 in groupers.

The hybrid grouper, a hybrid species, originates from *Epinephelus lanceolatus* ♂ and *Epinephelus fuscoguttatus* ♀ (Ch'ng and Senoo, 2008). With the rapid growth of the grouper farming industry, the delicious meat and unique nutritional content, this product has an important market value and is widely farmed in Southeast Asia and China (Liu et al., 2020). Groupers are predominantly farmed in the subtropical and tropical regions of South China, characterized by higher temperatures and humidity (Bureau of Fisheries of MARA, 2020; Wang et al., 2016). The hybrid grouper serves as an exemplary model for investigating the risks posed by AFB1 to fish. In recent years, there has been a gradual increase in the application of combined transcriptomic and metabolomic analyses in aquatic organisms for meat quality (Du et al., 2021), body coloration (Zhu et al., 2021), low-temperature tolerance mechanisms (Tu et al., 2023), and additives (Zhang et al., 2022). However, relatively few studies have been conducted on hybrid groupers exposed to AFB1 using a combined transcriptomic and metabolomic analysis approach.

The choice of dose in this experiment was based on the results of previous experiments, our previous experimental results found that the 96-h LD50 of AFB1 in groupers was 2 mg/kg body weight (Fig. S1), therefore, we designed 6 groups of feeds with diet AFB1 levels ranging from 7 to 2230 μg/kg, and the culture period was 56 days, and the experiments demonstrated that the dose ranging

between 445 and 2230 μg/kg did not affect the survival but significantly reduced the body weight and liver size of groupers (Liu et al., 2023). Therefore, the control group, the 445 μg/kg group, and the 2230 μg/kg group were selected as the focus of the study on the subacute exposure of hybrid groupers to AFB1, and the liver transcriptome and metabolome of groupers were jointly analyzed. By examining the mechanisms of liver damage induced by dietary AFB1 in hybrid groupers via histopathology of liver tissue, serum markers of liver injury, and a combined analysis of transcriptomics and metabolomics, this study aims to contribute to the understanding of how the aquaculture industry can maintain its stability and health.

2. Materials and methods

2.1. Animal ethics statement

All animal studies strictly followed the National Institutes of Health "Guide for the Care and Use of Laboratory Animals" and were approved by the Guangdong Ocean University Animal Ethics Committee (ID: GDOU-IACUC-2022-A0502, dated May 2, 2022). The procedures also met the ARRIVE guidelines (Percie du Sert et al., 2020).

2.2. Experimental diet preparation, feeding trial, and sample collection

Table 1 displays the basal diet composition. Dietary protein sources include brown fish meal, soy protein concentrate, wheat gluten, and chicken meal. Fish oil and soybean lecithin were used as sources of dietary lipids. High-purity (over 99%) AFB1 was sourced from Pribolab in Singapore. AFB1 was first dissolved in 2 mL of heated chloroform, followed by the addition of 50 mL fish oil after complete dissolution. Afterward, the temperature of the water bath in the fume hood was set to 62 °C. The amalgamated fish oil was placed in the water bath, facilitating the total volatilization of chloroform. The fatty acid composition of fish oil and AFB1-contaminated fish oil is given in Table S1. Afterward, the AFB1-contaminated fish oil was added to the fresh fish oil in a specific ratio, ensuring complete blending with the raw materials during the process of creating the diet. This resulted in final concentrations of 7 (AF7), 30 (AF30), 111 (AF111), 445 (AF445), and 2230 μg/kg of AFB1 (AF2230) in the diet (Table S2) (Liu et al., 2023). The control group was given a basic diet without any AFB1 added. The diet ingredients were crushed through 60 mesh sieve, weighed according to the formula proportion of various raw materials for mixing, a small number of components using a step-by-step expansion method of mixing, put into the V-type vertical mixer mixing, and then add fish oil and soy lecithin, the oil particles rubbed loose through 40 mesh sieve, slowly add about 30% of the weight of the diet water with a mixer and mix again, with the F-26 Twin Screw Extruder (South China University of Technology, Guangzhou, China), pelletizing, diet pellet size 3 to 4 mm. After drying, the diet was packed in sealed bags and stored in the refrigerator at −20 °C for use (Liu et al., 2021). The AFB1 concentration in the diet was assessed by NY/T 2071-2011. Briefly, according to the method of NY/T 2071-2011, a 5-g of diet sample was weighed in a 50-mL centrifuge tube, accurately added 25 mL of extraction solution (accurately measure 840 mL of acetonitrile and 160 mL of water, shaking). The mixture was vortexed and mixed for 2 min, and was placed in an ultrasonic cleaner and ultrasonic extraction for 20 min, with intermediate vibration for 2 to 3 times. Subsequently, the sample was retrieved and centrifuged at 6224 × *g* for 5 min. The supernatant was then transferred into a separatory funnel, and 15 mL of hexane was added, followed by thorough mixing. After phase separation, 5 mL of the sample was taken and passed through a multifunctional purification column (Mycotoxin Multifunctional Purification Column: Trilogy T °C-M160 column), with a flow rate controlled at 1 mL/min. The eluent was collected and evaporated to dryness under a stream of nitrogen gas at 50 °C. The residue was dissolved in 1.0 mL of acetic acid in acetonitrile solution (0.2% acetic acid + acetonitrile = 10 + 90, vol:vol), vortexed for 30 s, and filtered through a 0.22-μm filter membrane (Jinteng, Tianjin, China), followed by analysis using liquid chromatography-tandem mass spectrometry (LC–MS/MS). The LC–MS/MS system utilized was an Agilent 1290-6470 ultra-high-performance liquid chromatography–tandem mass spectrometer (Agilent, Technologies, Santa Clara, CA, USA), equipped with a ZORBAX SB-C18 column (Agilent, Technologies, Santa Clara, CA, USA), 1.8 μm, 2.1 × 100 mm in dimensions. The mobile phase consisted of: phase A, a 0.2% aqueous acetic acid solution; phase B, acetonitrile, with a gradient elution program as follows: 0 to 2 min, 15% B; 2 to 5 min, 15% B increasing to 30% B; 5.1 to 6 min, 100% B; 6.1 to 8 min, returning to 15% B. The column temperature was maintained at 30 °C, and the injection volume was 3 μL. Mass spectrometry conditions were as follows: ion source, electrospray ionization source (ESI^+); monitoring mode, multiple reaction monitoring; capillary voltage, 4000 V; drying gas flow rate, 7 L/min; drying gas temperature, 300 °C; sheath gas flow rate, 11 L/min; sheath gas temperature, 350 °C. Additional mass spectrometry acquisition parameters are detailed in Table S3.

The indoor flow-through aquaculture system used in this experiment was provided by Zhanjiang Evergreen South Marine Science & Technology Co., Ltd. Juvenile groupers were sourced from Hongyun Fishery (Zhanjiang, China). After a two-week experimental environmental adaptation period, hybrid grouper larvae were randomly assigned to 18 fiberglass tanks, each with a volume of

Table 1
Composition and nutrient levels of the basal diet (dry matter basis, %).

Item	Content
Ingredients	
Brown fish meal	43.00
Soybean protein concentrate	13.00
Wheat gluten	6.00
Chicken meal	11.00
Wheat flour	15.00
Soybean lecithin	1.50
Fish oil	3.00
Calcium dihydrogen phosphate	1.00
Choline chlorine	0.50
Vitamin and mineral premix[1]	1.00
Microcrystalline cellulose[2]	4.82
Antioxidant[3]	0.03
Attractant[4]	0.15
Total	100.00
Nutrient levels[5]	
Dry matter	92.23
Crude protein	49.03
Crude lipid	9.20
Ash	9.73

[1] Vitamin and mineral premix contained (per kilogram of diet): thiamine 5 mg, riboflavin 10 mg, vitamin A 5000 IU, vitamin E 40 mg, vitamin D_3 1000 IU, menadione 10 mg, pyridoxine 10 mg, biotin 0.1 mg, cyanocobalamin 0.02 mg, calcium pantothenate 20 mg, folic acid 1 mg, niacin 40 mg, vitamin C 150 mg, iron 100 mg, iodine 0.8 mg, copper 3 mg, zinc 50 mg, manganese 12 mg, selenium 0.3 mg, cobalt 0.2 mg.
[2] Purchased from Linchen Medical Technology Co., Ltd. (Shanghai, China).
[3] Purchased from Bangcheng Biological Engineering Co., Ltd. (Shanghai, China).
[4] Purchased from Hangzhou King Techina Technology (Hangzhou, China).
[5] Measured values.

500 L. A total of 540 hybrid groupers (average weight 11.59 ± 0.03 g) were divided into six treatments. The control group was fed a basal diet, and the five treatment groups were fed a basal diet containing 7 (AF7), 30 (AF30), 111 (AF111), 445 (AF445), and 2230 μg/kg AFB1 (AF2230) (Table S2), with three replicates per group and 30 fish per replicate. Groups C, AF445, and AF2230 were finally selected for subsequent trials based on growth data and serum biochemical indices through feeding trials (Liu et al., 2023). After half an hour of feeding, the unconsumed diet was siphoned off and collected for drying while a major water change was carried out. When the water was almost full, the water quality was maintained with 730 mL/min of flowing water with continuous aeration. Seawater pH, temperature, and dissolved oxygen (DO) were measured 3 times a day (08:00, 16:00 and 22:00). In the experiment, pH and water temperature were recorded at 7.4 ± 0.3 °C and 29.5 ± 2.0 °C, respectively, with DO levels over 6.0 mg/L. The pH level was measured with a TP110 (TIMEPOWER, Beijing, China), temperature with a thermometer (ZhongXing Glass Gage Factory, Hengshui, China), and DO with an Orion Star A213 RDO/ODO (Thermo Fisher Scientific, Waltham, MA, USA). The experiment used natural light and dark cycles. Growth-related indices were calculated by weighing fish in each fiberglass tank before and after the trial.

At the end of the experiment, the hybrid groupers were starved for 24 h. The fish were anaesthetized using eugenol (1:10,000) and then weighed and counted. Three fish per bucket were randomly chosen and measured for length, weight, and the weight of viscera and liver, following the method by Liu et al. (2023). The livers of these three fish were then rinsed with saline and then cut into soybean-sized pieces with a scalpel and preserved in 4% paraformaldehyde for histopathological examination. Then 12 fish were randomly selected from each fiberglass bucket and their livers were taken, the livers were cut into mung bean size with ophthalmic scissors, and small pieces of liver from three different fish were randomly selected and mixed into one enzyme-free freezing tube, for a total of 12 enzyme-free tubes, which were then quickly transferred to liquid nitrogen for rapid freezing, and these livers were subsequently used for real-time fluorescence quantification, liver transcriptome, and liver metabolome assays. Finally, six fish were randomly selected from each tank, and their blood was collected into 1.5 mL EP tubes, which were precipitated overnight at 4 °C, and then centrifuged at 3000 × *g* to extract clear serum for the determination of biochemical indexes.

2.3. Growth performance

Refer to Liu et al. (2023) for the determination indexes and methods of growth performance. In this experiment, Z-score normalization is used to analyze the data of growth performance. Calculation formula of growth indices were as follows:

Survival rate (SR, %) = 100 × final fish number/initial fish number;

Hepatosomatic indices (HSI, %) = 100 × liver wet weight (g)/body wet weight (g);

Viscerosomatic index (VSI, %) = 100 × viscera wet weight (g)/body wet weight (g).

2.4. Determination of proximate nutrient contents and biochemical indicators

The Association of Official Analytical Chemists (AOAC, 2006) methods were used to determine dry matter (dried at 105 °C, GRX-9203A, Shanghai, China) (method 934.01), crude protein (by Kjeldahl apparatus, nitrogen × 6.25, K9840, Shanghai, China) (method 976.05), crude lipid (extraction with petroleum ether by Soxhlet apparatus, KANGDA, Yancheng, China) (method 920.29), and ash (by combustion in muffle furnace at 550 °C, DP-SX-8-10, Beijing, China) (method 942.05) in raw materials, whole-body, diets, and muscle. Serum biochemical indices were measured for total protein (TP), albumin (ALB), alanine aminotransferase (ALT), aspartate aminotransferase (AST), and triglycerides (TG), and the detailed data are shown in previously published papers (Liu et al., 2023). Muscle and liver AFB1 content was determined using Pribolab EKT-010Q (Pribolab Pte. Ltd. Singapore) AFB1 enzyme-linked immunosorbent assay (ELISA) kit.

2.5. Liver histological observation and muscle fatty acids

The technique of Liu et al. (2021) was applied. Liver samples were fixed in Bouin's solution for 24 h, then preserved in 70% ethanol and embedded in paraffin after ethanol dehydration. Hematoxylin-and-eosin (H&E) − stained 5 to 7 μm slices were examined with a Nikon ECLIPSE 80i microscope (Nikon Corporation, Kanagawa, Japan). Pathological criteria were from Bu and Li (2018). Fatty acid methyl esters, derived from total lipids via acid-catalyzed transmethylation with boron trifluoride-methanol, were analyzed by gas chromatography (7890A, Agilent Technologies, Santa Clara, CA, USA).

2.6. Metabolomics data analysis

Non-targeted metabolomics was performed on 18 tissue samples (6 from Control, 6 from AF445, and 6 from AF2230). Mix 50 mg of tissue with 1000 μL of extraction solvent containing internal standards (20 mg/L, methanol:acetonitrile:water volume ratio = 2:2:1); vortex for 30 s. To extract metabolites, the following steps were followed: 1) add steel balls, process with a 45-Hz grinder for 10 min, and sonicate for 10 min in an ice-water bath; 2) let the samples stand at −20 °C for 1 h; 3) centrifuge at 4 °C, 14,005 × *g* for 15 min; 4) carefully remove 500 μL of the supernatant into an EP tube; 5) dry the extract in a vacuum concentrator; and 6) re-dissolve the dried metabolites with 160 μL. to the following steps were used to prepare QC samples for machine detection: 1) vortex for 30 s and sonicate in ice-water bath for 10 min; 2) centrifuge samples at 4 °C, 14,005 × *g* for 15 min; and mix 10 μL of each sample with 120 μL of supernatant in a 2-mL injection vial. The metabolomics LC–MS system used a Waters Acquity I-Class PLUS ultra-high-performance liquid chromatography (UHPLC) coupled with a Waters Xevo G2-XS QTOF high-resolution mass spectrometer and a Waters Acquity UPLC HSS T3 column (1.8 μm, 2.1 × 100 mm). The raw data from MassLynx V4.2 were processed using Progenesis QI software for peak extraction, peak alignment, and other data processing operations, and identification was done using the online METLIN database, public databases, and a proprietary Biomax database with theoretical fragment identification and mass deviations of 100 ppm for parent ions and 50 ppm for fragment ions. Quality control-based robust LOESS signal correction (QC-RLSC) corrects batch effects. Principal component analysis (PCA) and partial least square discriminant analysis (PLS-DA) were used for dimensionality classification analysis to analyze sample clustering and dispersion. Metabolites with differential expression between groups were identified using PLS-DA, with variable importance in projection (VIP) ≥ 1, *P*-value < 0.05, and ratio ≥2 or ≤1/2.

2.7. Transcriptomics analysis

Total RNA from animals was extracted using the TRIzol reagent (Life technologies, Carlsbad, CA, USA) and measured for concentration and purity with the NanoDrop 2000 (Thermo Fisher Scientific, Wilmington, DE, USA). The RNA Nano 6000 Assay Kit on the Agilent Bioanalyzer 2100 (Agilent Technologies, Santa Clara, CA, USA) assessed RNA integrity. Sequencing libraries were made with the NEBNext Ultra RNA Library Prep Kit (NEB, Massachusetts, USA) and purified using the AMPure XP System (Beckman Coulter, Beverly, USA). Libraries were sequenced using Illumina technology, yielding 5.88 Gb of data per sample. Raw reads were processed with the BMKCloud (www.biocloud.net) online bioinformatics tool. Filtered sequencing data were used for analysis. Adapter sequences were deleted using Cutadapt (Martins et al., 2011), and low-quality sequences like polyA-T and truncated sequences shorter than 100 bp were eliminated using fqtrim. Next, FastQC (http://www.bioinformatics.babraham.ac.uk/projects/fastqc/) confirmed sequence quality, including clean data Q20, Q30, and GC content. Trinity 2.4.0 assembled the transcriptome for this experiment (Grabherr et al., 2011). Gene functions were annotated utilizing databases such as National Center for Biotechnology Information (NCBI)'s Nr and Nt, Pfam for protein families, Clusters of Orthologous Groups of proteins (KOG/COG) for orthologous protein groups, Swiss-Prot for curated protein sequences, Kyoto Encyclopedia of Genes and Genomes (KEGG)'s KEGG Orthology (KO) for orthologs, and Gene Ontology (GO) for gene ontology. We defined differentially expressed genes (DEG) as significant if they had an false discovery rate (FDR) of less than 0.01 and a fold change of 1.5 or higher. The KEGG Orthology Based Annotation System (KOBAS) software was employed to statistically evaluate the enrichment of these DEG within KEGG pathways (Mao et al., 2005). Raw transcriptome sequence data are stored at the China National Centre for Bioinformation under accession number CRA014532.

2.8. Real-time quantitative PCR (RT-qPCR) validation of differentially expressed genes

Ten differentially expressed genes in the AF445 and AF2230 groups were randomly selected for RT-qPCR to verify the RNA-Seq data (Table 2). Total liver RNA was extracted using a universal RNA extraction kit and electrophoresed on a 1.2% denaturing agarose gel to determine integrity. The NanoDrop 1000 (Thermo Scientific, Delaware, USA) spectrophotometer assessed RNA quality and integrity. First-strand cDNA was synthesized in RT using the PrimeScript RT-PCR Kit (TaKaRa, Shiga, Japan) per the manufacturer's instructions. Data acquisition was performed every 6 s; therefore, the heat treatment program consisted of 40 cycles of 30 s at 95 °C, 5 s at 95 °C, and 34 s at 60 °C, as well as a stepwise melting curve step from 60 to 95 °C at a rate of 0.5 °C/s. The cDNA loads were normalized using β-actin and 18S ribosomal RNA (*18s*) as reference genes based on preliminary experimental results of internal control gene evaluation. Gene expression results were analyzed according to the $2^{-\Delta\Delta Ct}$ method of Livak and Schmittgen (2001).

2.9. Integrated analysis of metabolomics and transcriptomics

To study genes–metabolites relationships, all DEG and differential metabolites (DM) were mapped to the KEGG pathway database in Control vs AF445 and Control vs AF2230 pairwise comparisons. Altered pathways were found using KEGG pathway enrichment. Using BMKCloud (www.biocloud.net), interaction route diagrams of differentially expressed genes and metabolites during AFB1 exposure showed the link between DEG and DM.

2.10. Data analysis

Data of growth indices were Z-score normalization using Microsoft Excel 2019, Z-score normalization using the following formula: $Xnorm = X - \mu/\sigma$, where μ is the mean of the data and σ is the standard deviation of the data.

Whole fish and muscle crude lipid, and liver AFB1 content were analyzed by one-way ANOVA using IBM SPSS Statistics 16 (IBM Corp., Armonk, NY, USA), Analyses of normality and homology were performed before applying ANOVA. Multiple comparisons of means were performed using Tukey's HSD test when significant differences were found between groups. $P < 0.05$ was considered as significant difference. All data are expressed as mean or mean ± standard error of the mean (SEM).

3. Results

3.1. Growth index and serum biochemical indices

Figure 1 presents the Z-score normalized growth indices of groupers fed different concentrations of AFB1 in diets for 8 weeks. Specific growth indicator data can be found in previously published articles (Liu et al., 2023). A decline in final body weight (FBW), HSI, and VSI was observed, with the lowest values corresponding to a dietary AFB1 concentration of 2230 μg/kg. The respective R^2 values for FBW, HSI, and VSI were 0.9464, 0.7073, and 0.7065. Survival rate was unaffected by AFB1 concentration, with an R^2 value of 0.0411, likely due to the limited variability in the data (93.33% and 96.67%), resulting in a poor fit.

Table 2
Sequences of the primer pairs used for real-time quantitative PCR.

Gene	Forward primer (5′ to 3′)	Reverse primer (5′ to 3′)	Amplicon, bp	Amplification efficiency, %	Genbank no.
fas	GGCAGAGAGGACAACAGTAAAG	GTGTCAGGGTTCAGGCTATTT	108	92	XM_049563855.1
ppar-γ	GACAAGAATCGGAGGATGAGAG	ACACAACAGAGCACCAAGAG	107	95	XM_033627074.1
lpl	AGAAGACAACATGAGCCGTAAA	AGAGTTGTTCTGCCCGTAAAG	79	96	XM_033622741
gpx4a	TCCTCTGTGGAAGTGGCTGA	TCATCCAGGGGTCCGTATCT	132	94	XM_033622197.1
fads2	GCCTTACAGTGTCTTGAAC	ACAGAAGCAGAGCAGAAC	192	97	XM_033635131.1
jam2b	CGACCTCATTAGATACTCCAT	CGTCAGATTCACAGGATACT	176	98	XM_033618004.1
foxo4	GGGAGATACAAGGGAAGCAGTAACAC	GCGGTGGTCAGCTTGATGTCTC	86	98	XM_050041589
rasgef	ACCAGACCAAGGAGGAAG	AGCAGGAATGTGAAGATGTA	142	94	XM_033619279.1
aoc1	AGACAAGCCATTCCAATACA	AAGACACAACATCTGACCAT	163	96	XM_033638253.1
srebf1	TGTGGCTGCTCAACGGTATT	TGGGCGAAATCTCCTCTAGC	154	95	XM_033644260.1
β-actin	GGCTACTCCTTCACCACCACA	TCTGGGCAACGGAACCTCT	188	98	XM_033645256.1
18s	CGTATTGTGCCGCTAGAGGTGAA	TGGTGGTGCCCTTCCGTCAA	280	95	XR_007448850.1

fas = fatty acid synthase; *ppar-γ* = peroxisome proliferator-activated receptor-γ; *lpl* = lipoprotein lipase; *gpx* = glutathione peroxidase 4a; *fads2* = fatty acid desaturase 2; *jam2b* = junctional adhesion molecule 2b; *foxo4* = forkhead box o4; *rasgef* = rasgef domain family, member 1; *aoc1* = amine oxidase copper containing 1; *srebf1* = sterol regulatory element binding transcription factor 1; *18s* = 18S ribosomal RNA.

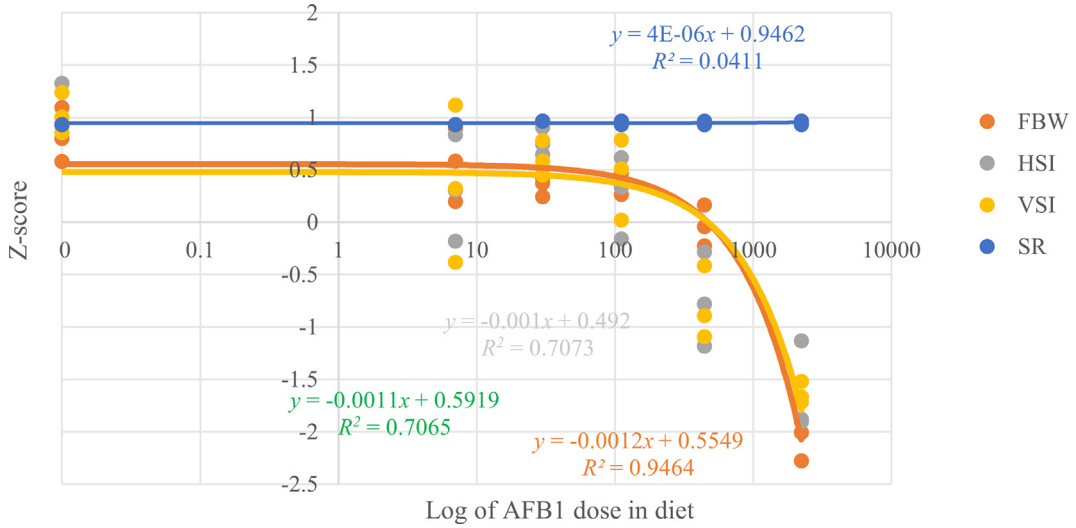

Fig. 1. Growth of hybrid groupers fed the experimental diets containing different aflatoxin B1 (AFB1) levels for 8 weeks. Diet AFB1 concentrations of 0, 7, 30, 111, 445, and 2230 μg/kg. This figure is the regression analysis after Z-score normalization of the original data. Z-score normalization formula is $Xnorm = X - \mu/\sigma$, where μ is the mean of the data and σ is the standard deviation of the data. FBW = final body weight; HSI = hepatosomatic index; VSI = viscerosomatic index; SR = survival rate.

Data on serum biochemical indices have been published in previous papers (Liu et al., 2023). The results showed that the mean values of ALB and TG were much smaller than those of the control group in the AF445 group and the AF2230 group ($P < 0.05$), whereas the mean values of ALT, AST, and LDH were much higher than those of the control group ($P < 0.05$).

Based on the growth and serum biochemical indices of the hybrid groupers, it was determined that liver damage occurred in the AF445 and AF2230 groups, therefore, the control, AF445 and AF2230 groups were selected for histological, muscle fatty acid, transcriptome and metabolome analyses.

3.2. Whole-body and muscle crude lipid, liver AFB1 content, and muscle fatty acids

Table 3 indicates that the crude lipid was significantly reduced in the AF2230 group in both whole-body and muscle tissues ($P < 0.05$) compare to the control group, while in the AF445 group, only muscle crude lipid levels were significantly decreased ($P = 0.001$). AFB1 was undetectable in the livers of the control group but was present in both the AF445 and AF2230 groups, with an increase correlating to higher dietary AFB1 intake.

Muscle fatty acid data are demonstrated in Table 4. Muscle total saturated fatty acids were significantly higher in both AF445 and AF2230 groups than in the control group ($P < 0.001$). Total monounsaturated fatty acids were significantly greater ($P < 0.001$) in the AF445 and AF2230 groups compared to the control group. Significantly higher total unsaturated and polyunsaturated fatty acid levels were found in the control group compared to the AF445 and AF2230 groups ($P < 0.001$).

3.3. Liver histopathology

The control group fed a basic diet displayed well-defined hepatocytes with a normal liver lobular structure (Fig. 2, Control). The AF445 diet induced initial hepatocyte atrophy, nuclear fragmentation, and eosinophilic degeneration, as well as abnormal hepatocyte morphology and arrangement, numerous instances of karyopyknosis, and mild liver inflammation (Fig. 2, AF445). The AF2230 diet led to atypical liver cell shapes and organization, indistinct cell boundaries, a mix of normal and pathological cells, and the presence of inflammatory cells causing localized necrosis (Fig. 2, AF2230). H&E section results at 200× magnification was published previously (Liu et al., 2023), with 400× magnification images presented herein.

3.4. Metabolite analysis

Using qualitative and quantitative methods, 15,778 peaks and 5194 annotated metabolites of hybrid grouper liver were discovered. The first two principal components PC1 and PC2, for these three groups were derived by removing extraneous information from the metabolic data matrix to minimize its dimensionality. The scatter plot in Fig. 3B shows that PC1 (30.59%) and PC2 (18.92%) contributed 49.51%. The Venn diagram showed 46 divergent metabolites between groups control and AF445, 541

Table 3
Whole-body and muscle crude lipid, and liver AFB1 content of hybrid groupers fed the experimental diets containing different AFB1 levels for 8 weeks.[1]

Item	Group			*P*-value		
	Control	AF445	AF2230	ANOVA	Linear	Quadratic
Whole-body crude lipid, % wet base	5.56 ± 0.171[a]	5.17 ± 0.198[a]	3.63 ± 0.131[b]	<0.001	0.132	0.960
Muscle crude lipid, % wet base	1.84 ± 0.065[a]	1.47 ± 0.032[b]	1.15 ± 0.072[b]	0.001	<0.001	0.052
Liver AFB1, μg/kg dry matter base	0.01 ± 0.000[a]	1.73 ± 0.409[b]	2.76 ± 0.466[c]	0.005	0.510	0.332

AFB1 = aflatoxin B1.
[a to c] Values in the same row with different superscripts indicate significant difference ($P < 0.05$).
[1] Group control fed a basal diet, group AF445 fed a basal diet containing 445 μg/kg AFB1 and group AF2230 fed a basal diet containing 2,230 μg/kg AFB1. Values in the table are means ± SEM ($n = 3$).

Table 4
Muscle fatty acids contents (% total fatty acids) of hybrid groupers fed the experimental diets containing different AFB1 levels for 8 weeks.[1]

Item	Group			*P*-value		
	Control	AF445	AF2230	ANOVA	Linear	Quadratic
C14:0	2.86 ± 0.015[a]	4.03 ± 0.021[c]	3.46 ± 0.010[b]	<0.001	<0.001	<0.001
C15:0	0.33 ± 0.017[a]	0.51 ± 0.005[b]	0.61 ± 0.021[c]	<0.001	<0.001	0.019
C16:0	24.08 ± 0.010[a]	35.41 ± 0.056[c]	32.65 ± 0.007[b]	<0.001	<0.001	<0.001
C17:0	0.69 ± 0.010[a]	0.88 ± 0.041[b]	1.08 ± 0.012[c]	<0.001	<0.001	<0.001
C18:0	7.96 ± 0.021[a]	12.22 ± 0.032[b]	13.42 ± 0.051[b]	<0.001	<0.001	0.002
C20:0	0.59 ± 0.016[a]	0.83 ± 0.058[b]	0.91 ± 0.031[c]	<0.001	<0.001	0.122
C22:0	0.32 ± 0.010[a]	1.00 ± 0.066[b]	1.23 ± 0.008[b]	<0.001	<0.001	0.308
C24:0	0.12 ± 0.017[a]	0.25 ± 0.048[b]	0.30 ± 0.032[c]	<0.001	<0.001	0.066
∑SAFA	33.75 ± 0.029[a]	50.59 ± 0.038[b]	49.54 ± 0.041[b]	<0.001	<0.001	<0.001
C16:1n7	3.91 ± 0.050[a]	4.95 ± 0.015[c]	4.56 ± 0.051[b]	<0.001	<0.001	<0.001
C17:1n7	0.28 ± 0.031[b]	0.19 ± 0.011[a]	0.28 ± 0.032[b]	<0.001	0.123	0.009
C18:1n9t	0.19 ± 0.033[a]	0.28 ± 0.031[b]	0.29 ± 0.022[c]	<0.001	<0.001	0.339
C18:1n9c	22.70 ± 0.029[a]	29.72 ± 0.047[b]	30.36 ± 0.018[c]	<0.001	<0.001	<0.001
C20:1n9	1.91 ± 0.018[a]	2.35 ± 0.016[b]	2.35 ± 0.052[b]	<0.001	<0.001	<0.001
C22:1n9	0.35 ± 0.006[a]	0.46 ± 0.007[b]	0.53 ± 0.037[c]	0.011	0.005	0.257
C24:1n9	0.47 ± 0.033[a]	0.66 ± 0.018[b]	0.79 ± 0.052[b]	0.007	0.003	0.129
∑MUFA	29.80 ± 0.031[a]	38.59 ± 0.082[b]	39.15 ± 0.091[b]	<0.001	<0.001	<0.001
C18:2n6t	0.17 ± 0.021[a]	0.19 ± 0.051[ab]	0.21 ± 0.012[b]	0.048	0.029	0.135
C18:2n6c	12.10 ± 0.028[b]	4.81 ± 0.018[a]	5.83 ± 0.052[a]	<0.001	<0.001	<0.001
C18:3n3	1.19 ± 0.038[b]	0.19 ± 0.008[a]	0.20 ± 0.031[a]	<0.001	<0.001	<0.001
C20:2	0.63 ± 0.048[b]	0.20 ± 0.042[a]	0.24 ± 0.016[a]	0.001	<0.001	0.021
C20:3n6	0.26 ± 0.054	–	–	–		
C20:3n3	0.15 ± 0.013	–	–	–		
C20:4n6	1.02 ± 0.018	–	–	–		
C20:5n3	8.04 ± 0.081[b]	0.41 ± 0.052[a]	0.37 ± 0.038[a]	<0.001	<0.001	<0.001
C22:6n3	9.46 ± 0.054[b]	0.37 ± 0.006[a]	0.37 ± 0.028[a]	<0.001	<0.001	<0.001
∑HUFA[2]	18.91 ± 0.052[b]	0.79 ± 0.042[a]	0.76 ± 0.038[a]	<0.001	<0.001	<0.001
∑PUFA	32.53 ± 0.621[b]	6.16 ± 0.064[a]	7.22 ± 0.032[a]	<0.001	<0.001	<0.001
Total fatty acids	99.94 ± 0.007[b]	99.86 ± 0.031[a]	100.00 ± 0.000[c]	<0.001	<0.001	<0.001

AFB1 = aflatoxin B1; ∑SAFA = total saturated fatty acid; ∑MUFA = total monounsaturated fatty acids; ∑HUFA = total highly unsaturated fatty acid; ∑PUFA = total polyunsaturated fatty acids.
[a to c] Values in the same row with different superscripts indicate significant difference ($P < 0.05$).
[1] Group control fed a basal diet, group AF445 fed a basal diet containing 445 μg/kg AFB1 and group AF2230 fed a basal diet containing 2230 μg/kg AFB1. Values in the table are means ± SEM ($n = 3$).
[2] The total sum of the fatty acids C20:3 n6, 20:3 n3, C20:4 n6, 20:5 n3, and 22:6n3.

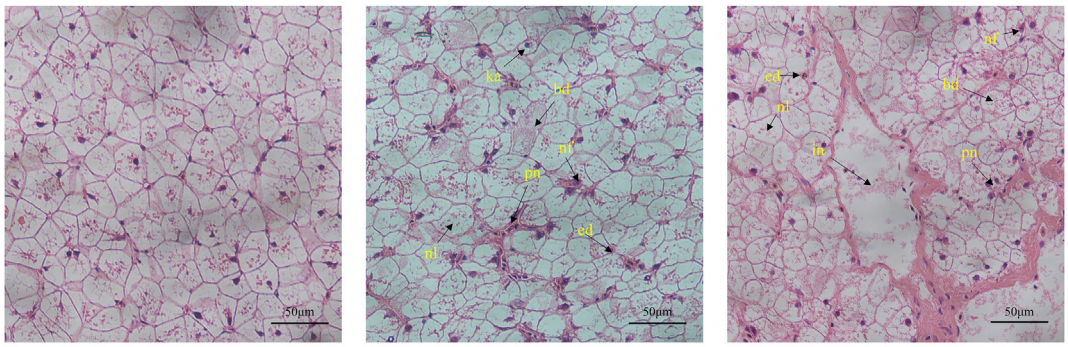

Fig. 2. Liver histology (magnification 400×) of juvenile groupers, fed diets differing in aflatoxin B1 (AFB1) levels. The images show: various signs of pathological change (marked using arrows). The numbers above the arrows indicate the type of damage present. Group control fed a basal diet, group AF445 fed a basal diet containing 445 μg/kg AFB1 and group AF2230 fed a basal diet containing 2230 μg/kg AFB1. ed = eosinophilic degeneration; nf = nuclear fragmentation; ka = karyopyknosis; nl = nuclear lysis; in = inflammation; sn = spotty necrosis; bd = ballooning degeneration.

between groups control and AF2230, and 38 in common (Fig. 3C). Orthogonal projections to latent structures-discriminant analysis (OPLS-DA) results (Fig. 4A and C) showed that groups Control's Q2 for Y (Q2Y) versus AF445 was 0.562 > 0.5, indicating an effective model, and that groups Control's Q2Y versus AF2230 was 0.905 > 0.9, indicating an excellent model. The OPLS-DA model may find and analyze differences between paired groups. The Q2Y fit regression line slope was positive for groups control versus AF445 and AF2230 in the permutation model used to validate the PLS-DA results, indicating that the model is meaningful (Fig. 4B and D). The blue dots generally above the red dots indicate good independence between the modeling training set and the test set. Of 46 DM in groups control versus AF445, 31 were higher in groups control and 15 in AF445 and 247 and 294 of the 541 DM were greater in groups control and AF2230, respectively (Fig. 5A and B). KEGG enrichment analysis was utilized to identify metabolic pathways linked to the changes. The KEGG enrichment map of different metabolites between groups control and AF445 showed cutin, suberin, and wax production as the most important route. Porphyrin, beta-alanine, tryptophan,

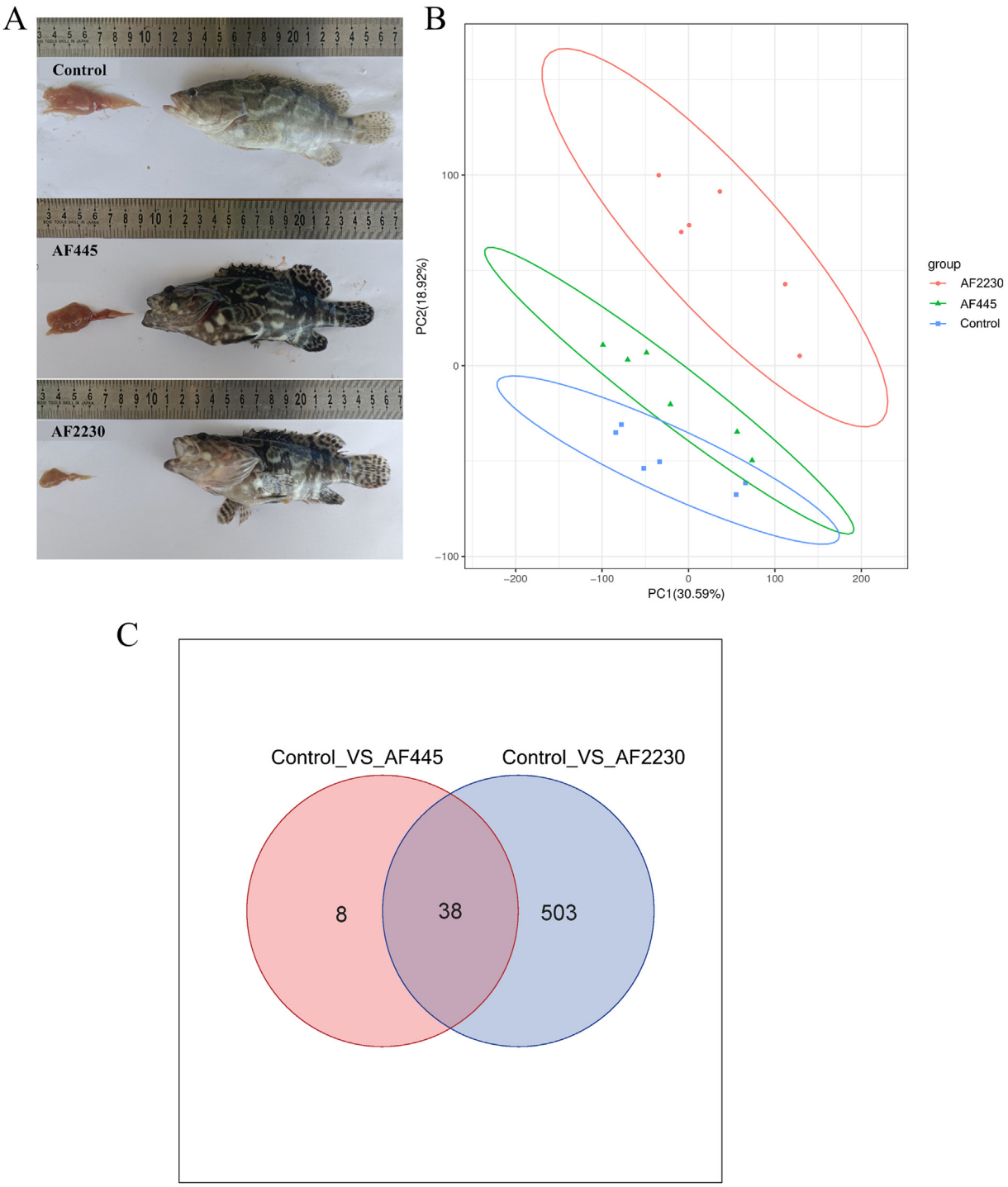

Fig. 3. Multivariate statistical analysis of metabolomics in hybrid grouper liver after 8 weeks of feeding diets containing different levels of aflatoxin B1 (AFB1). **(A)** Growth and liver size of groupers fed with different diets for 8 weeks. **(B)** Plot of ALL mode PCA score. **(C)** The Venn of DM distribution in three groups. Group control fed a basal diet, group AF445 fed a basal diet containing 445 μg/kg AFB1 and group AF2230 fed a basal diet containing 2230 μg/kg AFB1. PCA = principal component analysis; DM = differential metabolites.

and retinol metabolisms were likewise considerably enriched between the two groups (Fig. 6A). DM KEGG enrichment maps between groups control and AF2230 showed drug metabolism-cytochrome P450 as the most prominent route. Flavone and flavonol biosynthesis, cutin, suberin, and wax biosynthesis, steroid biosynthesis, beta-alanine metabolism, drug metabolism-other enzymes, and arginine and proline metabolism were found significantly enriched between the two groups (Fig. 6B).

3.5. Transcriptomic analysis

3.5.1. Transcriptome data sequencing and quality control

RNA-Seq raw data were filtered to 64.01 Gb of pure data. Transcriptome quality study showed that all individuals in groups control, AF445 and AF2230 had Q20 and Q30 over 99.99% and 92.74%, respectively. Table S4 shows that the data are high-quality and suitable for transcriptome expression analysis.

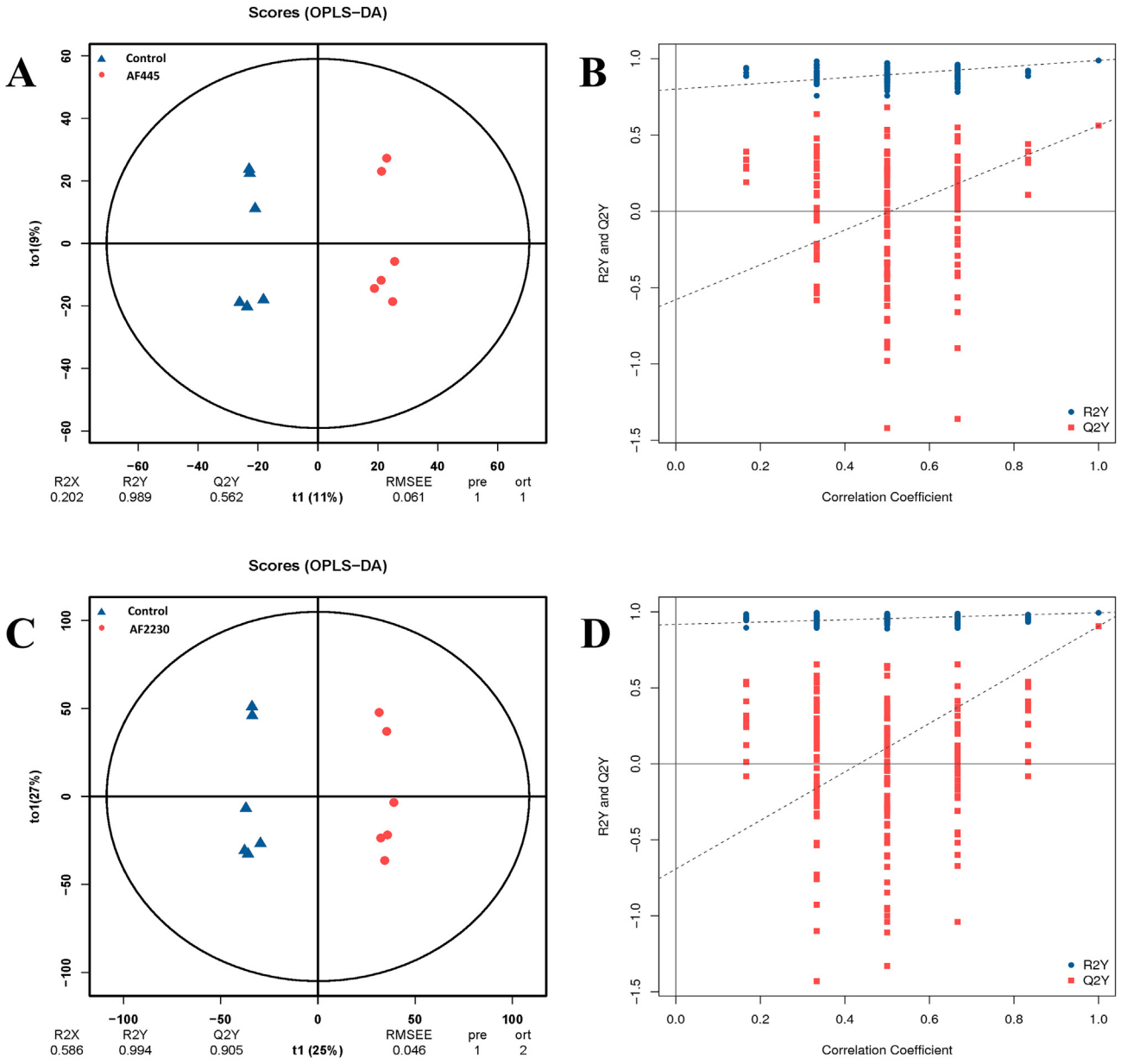

Fig. 4. Preliminary analysis of hepatic metabolomic profiles in hybrid groupers fed different diets for 8 weeks. **(A)** Control vs AF445 orthogonal projections to latent structures-discriminant analysis (OPLS-DA) test in the ALL mode; **(B)** Control vs AF445 orthogonal partial least-squares (PLS-DA) test in the ALL mode; **(C)** Control vs AF2230 PLS-DA test in the ALL mode; **(D)** Control vs AF2230 PLS-DA test in the ALL mode. Group control fed a basal diet, group AF445 fed a basal diet containing 445 μg/kg aflatoxin B1 (AFB1) and group AF2230 fed a basal diet containing 2230 μg/kg AFB1. RMSEE = root mean square error of estimate.

3.5.2. Identification of DEG between group control and AF445 and AF2230 groups and DEG was verified by RT-qPCR

The volcanic map showed DEG distribution in three groups (Fig. 7). The gene expression profiles of groups control, AF445 and AF2230 differed significantly. Out of 171 DEG (fold change > 1.5 and FDR < 0.01), 113 were up-regulated and 58 were down-regulated in group AF445 compared to group control (Fig. 7A). Out of 820 DEG found in groups control and AF2230 (fold change > 1.5 and FDR < 0.01), 464 were up-regulated and 356 were down-regulated compared to group control (Fig. 7B).

To confirm the precision of our transcriptome sequencing, we employed RT-qPCR to check 10 DEG from this research. Figure 8 displays the relative gene expression levels, aligning with the sequencing data. This consistency confirms the sequencing data's reliability.

3.5.3. GO and KEGG enrichment analysis of DEG

DEG were classified as biological process, cellular component, and molecular function. Cellular process, biological control, binding, and cellular anatomical entity dominate the three classifications (Fig. 9). To further comprehend the metabolic pathway variations between the control and experimental groups in KEGG, 82 DEG from groups control and AF445 were mapped to 102 metabolic pathways. Using a *P*-value < 0.01, 20 metabolic pathways were significantly enriched, including "metabolism" (drug metabolism-cytochrome P450, fatty acid metabolism, biosynthesis of unsaturated fatty acids, retinol metabolism, amino sugar and nucleotide sugar metabolism, metabolism of xenobiotics by cytochrome, tyrosine metabolism, histidine metabolism, drug metabolism-other enzymes, linoleic acid metabolism, pentose phosphate pathway) (Fig. 10A).

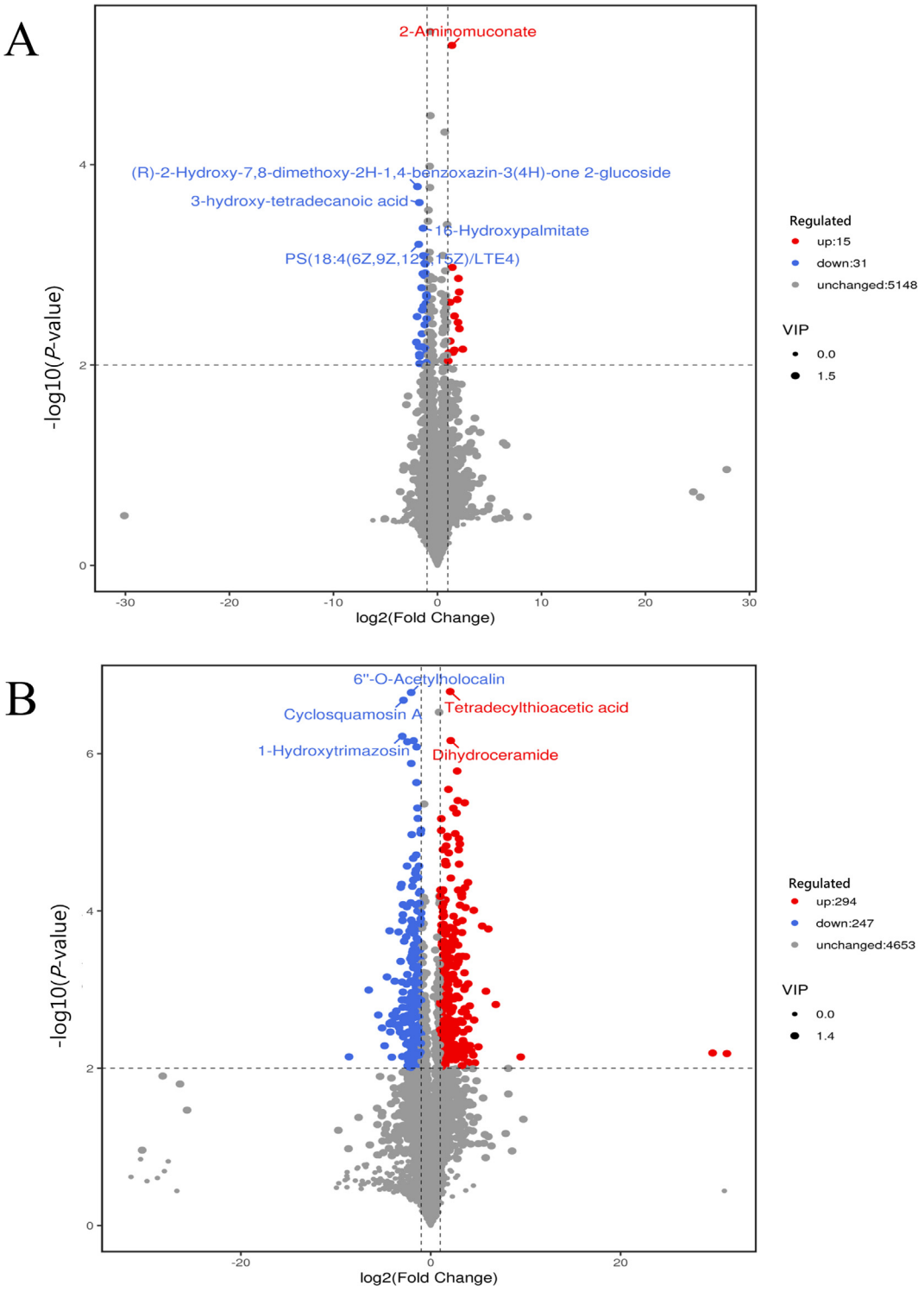

Fig. 5. Liver differential metabolite volcano plots of hybrid groupers fed different diets for 8 weeks. **(A)** Control vs AF445; **(B)** Control vs AF2230. Group control fed a basal diet, group AF445 fed a basal diet containing 445 μg/kg aflatoxin B1 (AFB1) and group AF2230 fed a basal diet containing 2230 μg/kg AFB1. VIP = variable importance in projection.

Overall, 347 DEG from groups control and AF2230 were linked to 171 metabolic pathways. Twenty of the most significantly enriched metabolic pathways were "metabolism" (metabolism of xenobiotics by cytochrome, retinol metabolism, drug metabolism-cytochrome P450, glycolysis/gluconeogenesis, carbon metabolism, tyrosine metabolism, fatty acid degradation, glycerolipid metabolism, pentose phosphate pathway, fructose and mannose metabolism, arginine and proline metabolism, biosynthesis of unsaturated fatty acids, beta-alanine metabolism, glutathione metabolism, biosynthesis of amino acids, foxo-signaling pathway) (Fig. 10B). This suggests hybrid grouper development involves many metabolic pathways. The KEGG bubble plot of upregulated DEG in groups control and AF445 showed that protein processing in endoplasmic reticulum was the most enriched pathway (Fig. 11A).

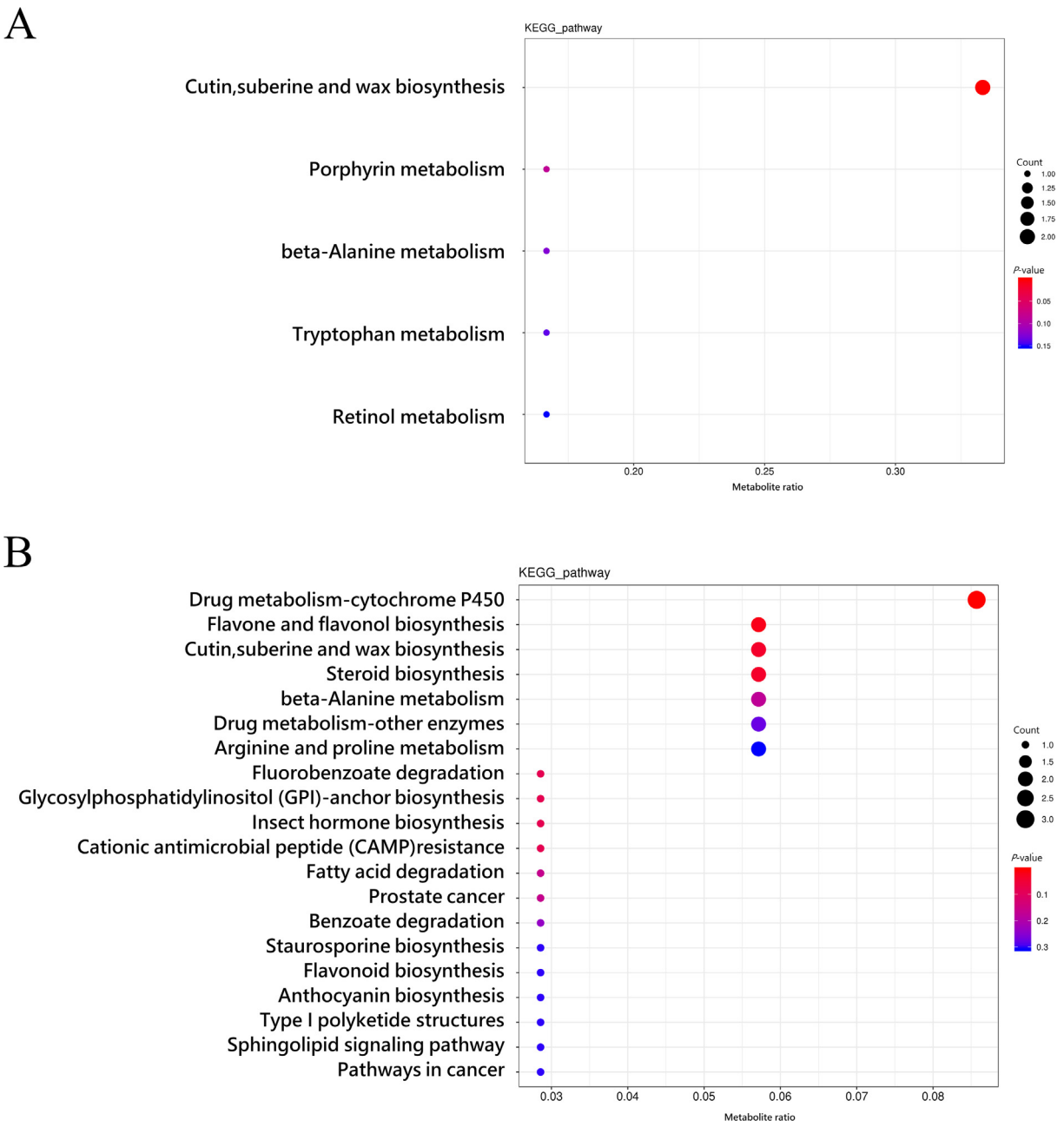

Fig. 6. KEGG enrichment analysis of differential metabolites in the liver of hybrid groupers fed different diets for 8 weeks. **(A)** Control vs AF445; **(B)** Control vs AF2230. Group control fed a basal diet, group AF445 fed a basal diet containing 445 μg/kg aflatoxin B1 (AFB1) and group AF2230 fed a basal diet containing 2230 μg/kg AFB1.

The KEGG bubble plot of elevated DEG in groups control and AF2230 showed that tight junction was the most enriched pathway (Fig. 11B). The KEGG bubble map of downregulated DEG in groups control and AF445 showed that drug metabolism-cytochrome P450 and fatty acid metabolism were highly enriched (Fig. 12A). The most enriched pathways in the KEGG bubble plot of downregulated DEG in groups Control and AF2230 were metabolism of xenobiotics by cytochrome and drug metabolism-cytochrome P450 (Fig. 12B).

3.6. Comprehensive analysis of metabolomics and transcriptomics

The thorough examination of the reaction of hybrid grouper livers to DEG and DM in response to two distinct amounts of AFB1 in the diet uncovered multiple enrichment pathways. The findings indicated that the response in groups control and AF455 was primarily associated with retinol metabolism, metabolism of xenobiotics by cytochrome, and drug metabolism-cytochrome P450. On the other hand, in group control with AF2230, the response was mainly linked to glycine, serine and threonine metabolism, sphingolipid metabolism, retinol metabolism, arachidonic acid metabolism, drug metabolism-cytochrome P450, α-linolenic acid metabolism, fatty acid degradation, and biosynthesis of unsaturated fatty acids (Fig. 13). Detailed DEG expression levels and DM levels for combined transcriptome and metabolome analyses are shown in Table S5 (control VS AF445) and Table S6 (control VS AF2230).

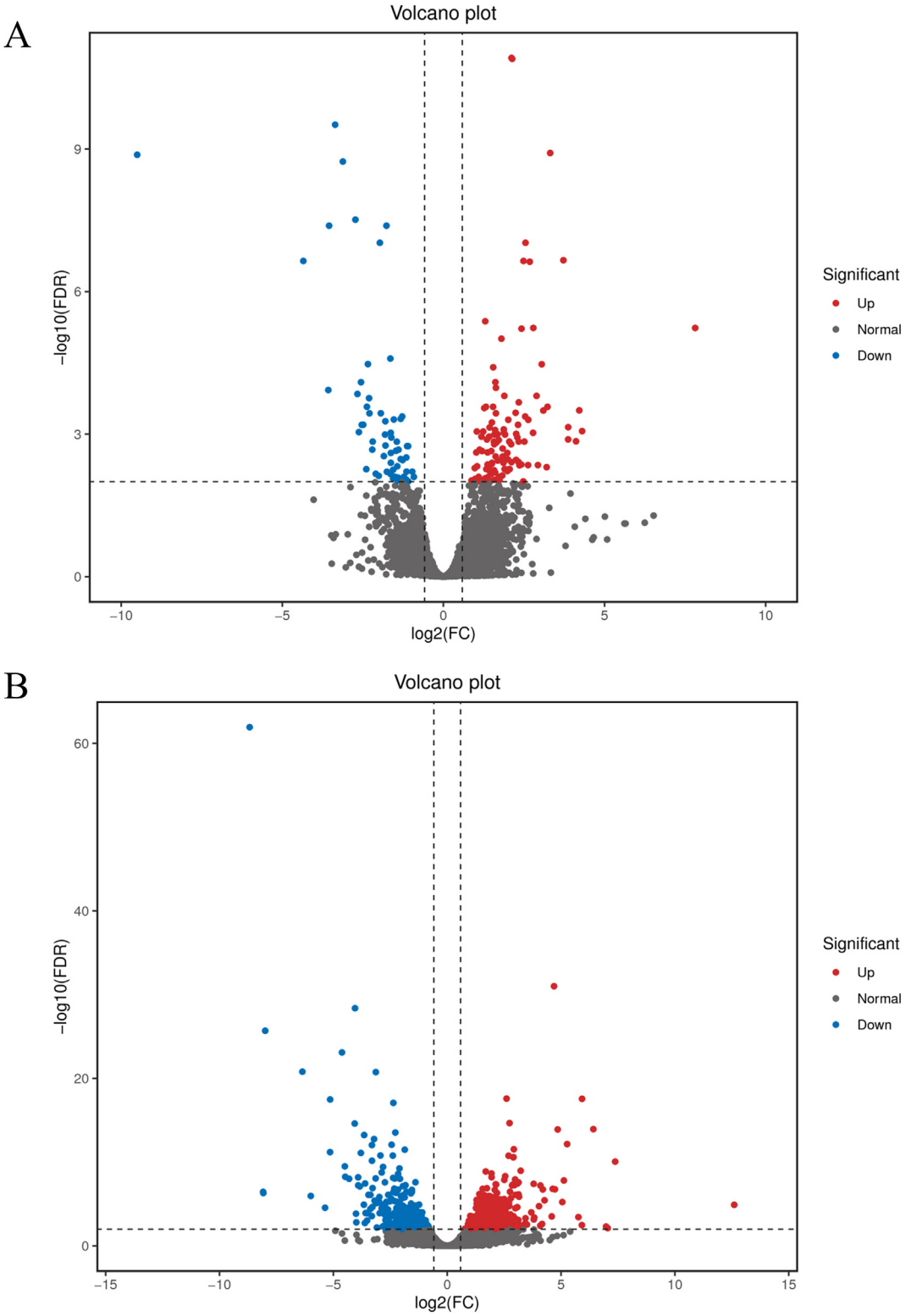

Fig. 7. Liver differential gene volcano maps of hybrid groupers fed diets with different aflatoxin B1 (AFB1) levels for 8 weeks. Volcano plot of DEG, red indicates the up-regulated gene expression level between two groups, blue indicates the down-regulated gene expression level between two groups, and gray indicated insignificant differential expression. **(A)** Control vs AF445; **(B)** Control vs AF2230. Group control fed a basal diet, group AF445 fed a basal diet containing 445 μg/kg AFB1 and group AF2230 fed a basal diet containing 2230 μg/kg AFB1. DEG = differentially expressed genes; FC = fold change; FDR = false discovery rate.

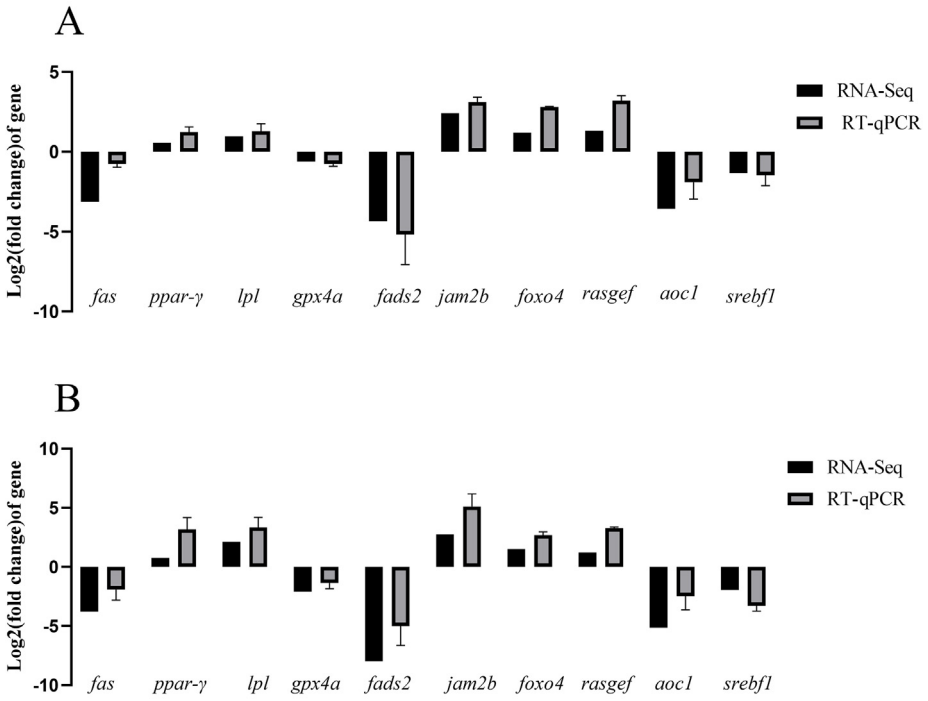

Fig. 8. Verification of related differential genes in liver of hybrid groupers. The x-axis indicates the names of candidate genes and the y-axis represents relative fold change. **(A)** Control VS AF445; **(B)** Control VS AF2230. Group control fed a basal diet, group AF445 fed a basal diet containing 445 μg/kg aflatoxin B1 (AFB1) and group AF2230 fed a basal diet containing 2230 μg/kg AFB1. *fas* = fatty acid synthase; *ppar-γ* = peroxisome proliferator-activated receptor-γ; *lpl* = lipoprotein lipase; *gpx* = glutathione peroxidase 4a; *fads2* = fatty acid desaturase 2; *jam2b* = junctional adhesion molecule 2b; *foxo4* = forkhead box o4; *rasgef* = rasgef domain family member 1; *aoc1* = amine oxidase copper containing 1; *srebf1* = sterol regulatory element binding transcription factor 1; RNA-Seq = RNA-sequencing; RT-qPCR = real-time quantitative PCR.

4. Discussion

The liver plays a crucial role in bioaccumulation, metabolism, and detoxification within organisms (Pérez-Acosta et al., 2016; Santangeli et al., 2018). Studies have demonstrated that AFB1 predominantly accumulates in hepatic tissues (Deng et al., 2010). In this study, it was observed that exposure to elevated concentrations (445 and 2230 μg/kg) of AFB1 resulted in increased hepatic accumulation and subsequent liver damage in groupers, aligning with previous research. ALT, AST, and LDH are pivotal enzymes for assessing liver function; their release into the bloodstream upon hepatocyte destruction indicates liver injury, with elevated serum levels serving as sensitive biomarkers of hepatic damage (Ali et al., 2017). Notably, serum biochemical results from the same culture experiment showed significantly higher serum ALT, AST, and LDH levels in the AF445 and AF2230 groups compared with the control group (Liu et al., 2023). It is hypothesized that this increase is attributable to substantial AFB1 accumulation in the liver, which disrupts hepatocyte integrity, enhances membrane permeability, and triggers hepatocyte necrosis. These observations corroborate the findings of Ayyat et al. (2018) and Abdelhiee et al. (2021).

Histopathology is a highly regarded technique for evaluating the detrimental impacts of pollutants on biological systems (Ali et al., 2017). The results of this study on liver H&E sections show that increasing AFB1 exposure leads to progressive morphological aberrations of hepatocytes, characterized by eosinophilic degeneration, nuclear fragmentation, karyopyknosis, nuclear lysis and ballooning degeneration, and increased inflammation. This pattern of hepatic damage under subacute AFB1 exposure is consistent with observations in tilapia subjected to 1641 μg/kg AFB1, which presented with necrotic lesions and hepatocellular vacuolation (Deng et al., 2010). Additionally, gibel carp (*Carassius auratus* gibelio) exposed to AFB1 within the range of 10 to 1000 μg/kg displayed hepatocellular vacuolation (Huang et al., 2011). Further, sea bream (*Sparus aurata*) exposed to 1 and 2 mg/kg of AFB1 exhibited signs of vacuolation, blood stasis, inflammatory infiltration, and hepatic necrosis (Barany et al., 2021). Collectively, the hepatic bioaccumulation data and histopathological assessments suggest that AFB1 exposure at intermediate and high concentrations (445 and 2230 μg/kg) can induce hepatic injury in hybrid groupers. Consequently, to elucidate the molecular underpinnings of AFB1-induced hepatic injury, groups administered with AFB1 at dosages of 445 and 2230 μg/kg, alongside a control group (0 μg/kg), were selected for transcriptomic and metabolomic profiling.

Retinol metabolism plays a crucial role in functions such as vision, antioxidant action, growth and development, and immunity (Blomhoff and Blomhoff, 2006). The results of the combined transcriptomic and metabolomic analyses in this experiment showed that both concentrations of AFB1 in the diet were enriched in the retinol metabolism pathway, with down-regulation of most of the differential genes and DM, suggesting that AFB1 in the diet may hurt liver retinol metabolism in groupers. Several studies have found that exposure to AFB1 affects the retinol metabolism pathway, which may lead to an increased incidence of vitamin A deficiency in the organism (Tang et al., 2009), and there have also been attempts to mitigate the toxicity of AFB1 on the liver through the addition of vitamin A or vitamin a precursor to the diet (Alpsoy and Yalvac, 2011; Cassand et al., 1993; Yu et al., 1994). However, the two concentrations of AFB1 diets in this experiment did not lead to a significant decrease in vitamin A in the liver, whereas upstream genes related to vitamin A metabolism were down-regulated, e.g., the expression levels of alcohol dehydrogenase 1/7 (*adh*) were decreased in both AF445 and AF2230 compared with the control

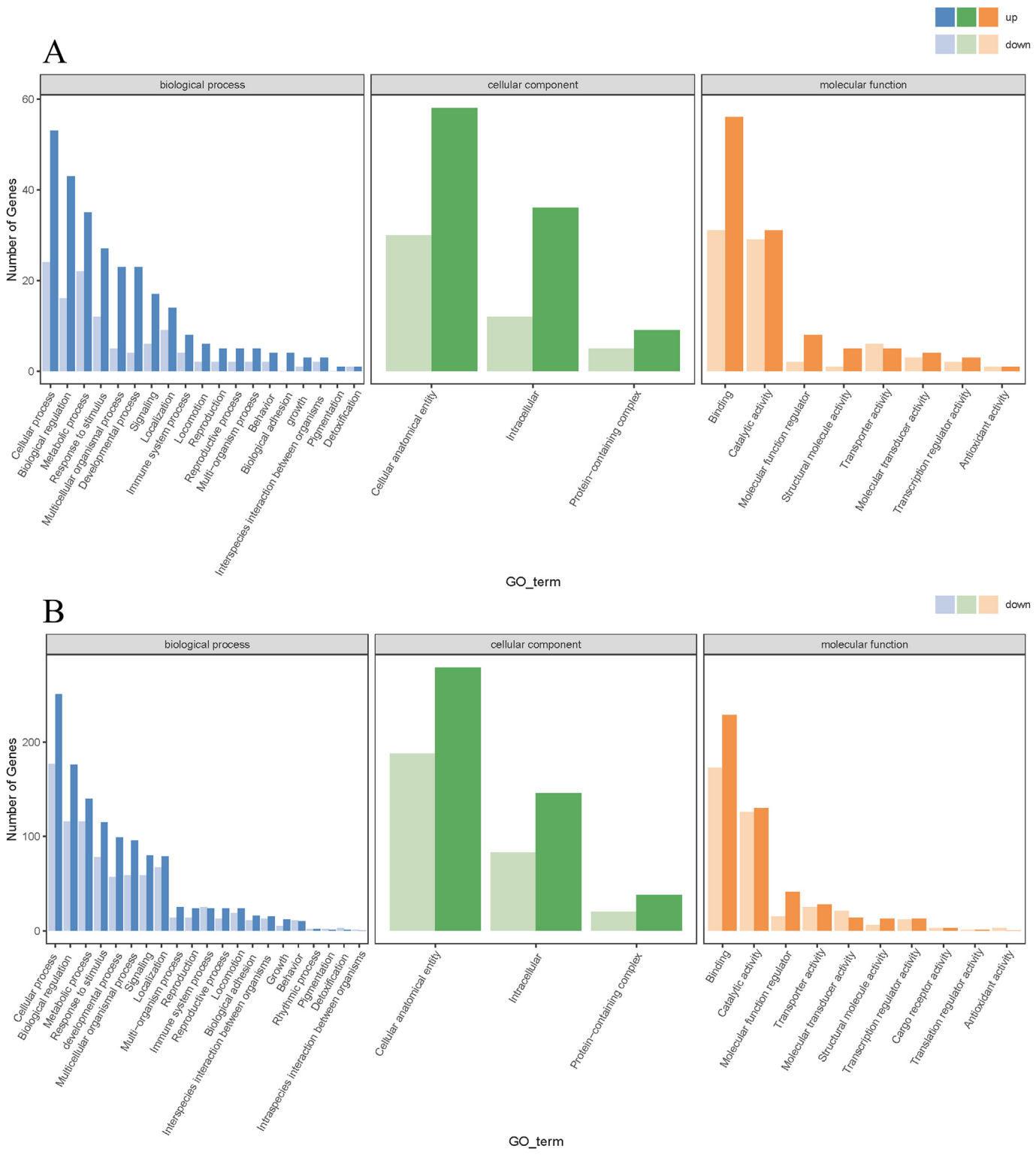

Fig. 9. Liver differentially expressed genes of hybrid groupers fed diets with different aflatoxin B1 (AFB1) levels for 8 weeks GO labeled classification statistics. x-axis: GO classification, y-axis: number of genes, different colors represent different primary classifications. **(A)** Control vs AF445; **(B)** Control vs AF2230. Group control fed a basal diet, group AF445 fed a basal diet containing 445 μg/kg AFB1 and group AF2230 fed a basal diet containing 2230 μg/kg AFB1.

group. This may be related to the fact that the liver can maintain stable vitamin A levels through a series of complex processes such as absorption, transport (Ghyselinck et al., 1999), storage, and metabolism (Blaner et al., 2016). Although AFB1 causes liver damage in hybrid groupers, this damage does not seem to be sufficient to change the relative vitamin A content in the liver. Additionally, there is no evidence for a direct association between AFB1 and adh, but the role of adh enzymes in maintaining intracellular redox balance and metabolizing substances such as alcohol may have an indirect effect on the overall cellular health and detoxification

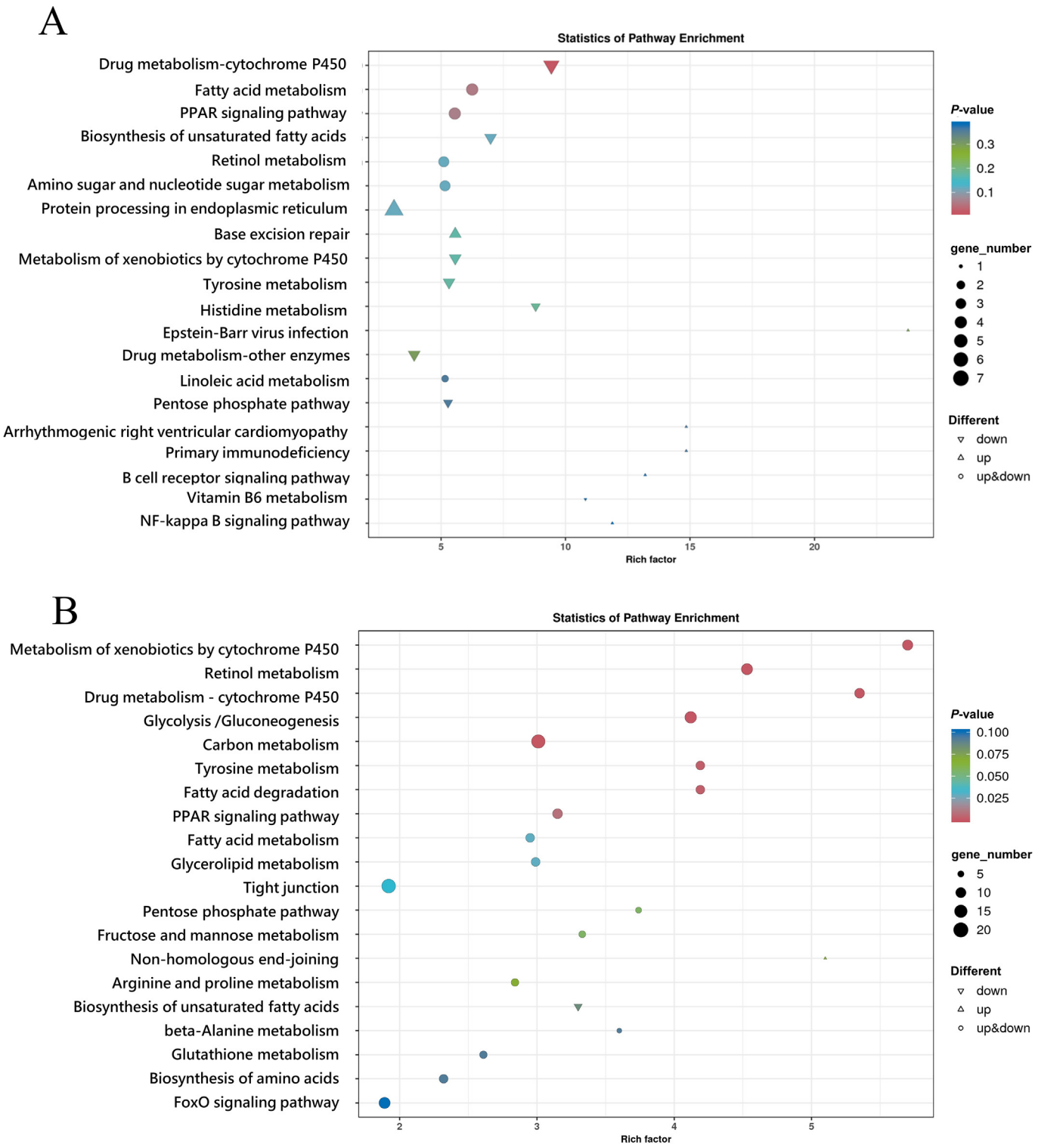

Fig. 10. KEGG bubble map (top 20) of DEG in hybrid groupers fed diets with different aflatoxin B1 (AFB1) levels for 8 weeks. **(A)** Control vs AF445; **(B)** Control vs AF2230. Group control fed a basal diet, group AF445 fed a basal diet containing 445 μg/kg AFB1 and group AF2230 fed a basal diet containing 2230 μg/kg AFB1. DEG = differentially expressed genes.

capacity. For example, adh enzyme activity may affect the intracellular reduced form of nicotinamide-adenine dinucleotide/oxidized nicotinamide adenine dinucleotide phosphoric acid ($NADH/NAD^+$) ratio (Masia et al., 2018), which, in turn, may affect the activity of cytochrome P450 (cyp450) enzymes, as these enzymes require NADPH as an electron donor when catalyzing reactions (Iyanagi et al., 2012). Compounds, such as 9-cis-retinal and 11-cis-retinal are derivatives of vitamin A where 11-cis-retinol is the alcohol form of 11-cis-retinal, play a key role in visual processes as an important component of visual pigmentation (Kono

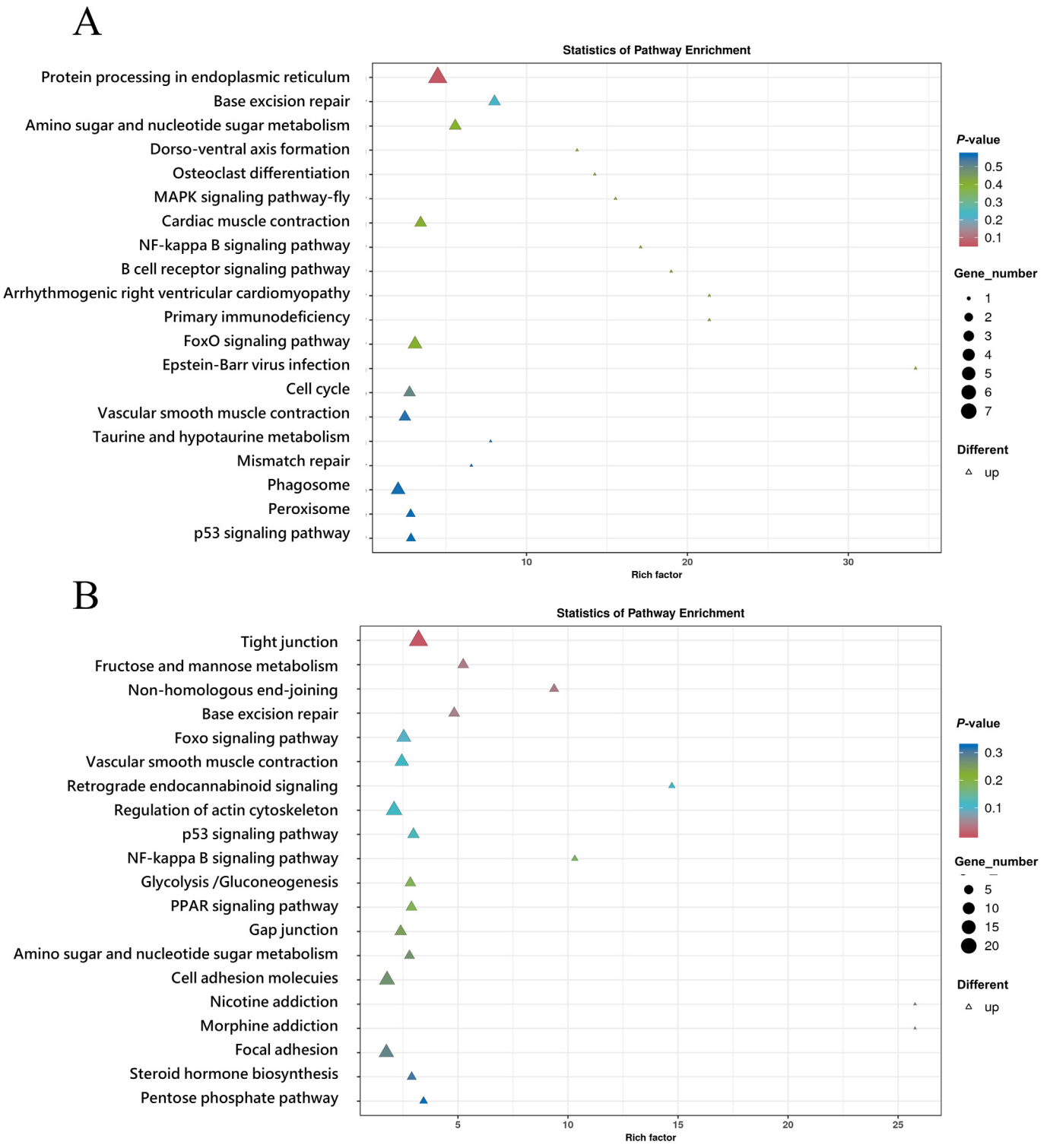

Fig. 11. KEGG bubble map (top 20) of up-regulated DEG in hybrid groupers fed diets with different aflatoxin B1 (AFB1) levels for 8 weeks. **(A)** Control vs AF445; **(B)** Control vs AF2230. Group Control fed a basal diet, group AF445 fed a basal diet containing 445 μg/kg AFB1 and group AF2230 fed a basal diet containing 2230 μg/kg AFB1. DEG = differentially expressed genes; MAPK: mitogen-activated protein kinases.

et al., 2008). In the present experiment, we found that 9-cis-retinal was down-regulated in both the AF445 and AF2230 groups, whereas 11-cis-retinal and 11-cis-retinol were down-regulated in AF445 and AF2230, respectively. Currently, there is no direct evidence that dietary AFB1 directly affects the levels or function of 9-cis-retinal, 11-cis-retinal, and 11-cis-retinol. However, since metabolites of AFB1 may cause damage to the liver and since the liver is a major site of vitamin A metabolism and storage (Blomhoff and Blomhoff, 2006), it is theoretically possible that AFB1 toxicity may indirectly affect the normal metabolism of vitamin A and the visual cycle. Since 9-cis-retinal was down-regulated in both AFB1 diet groups, we thought it could serve as a potential marker.

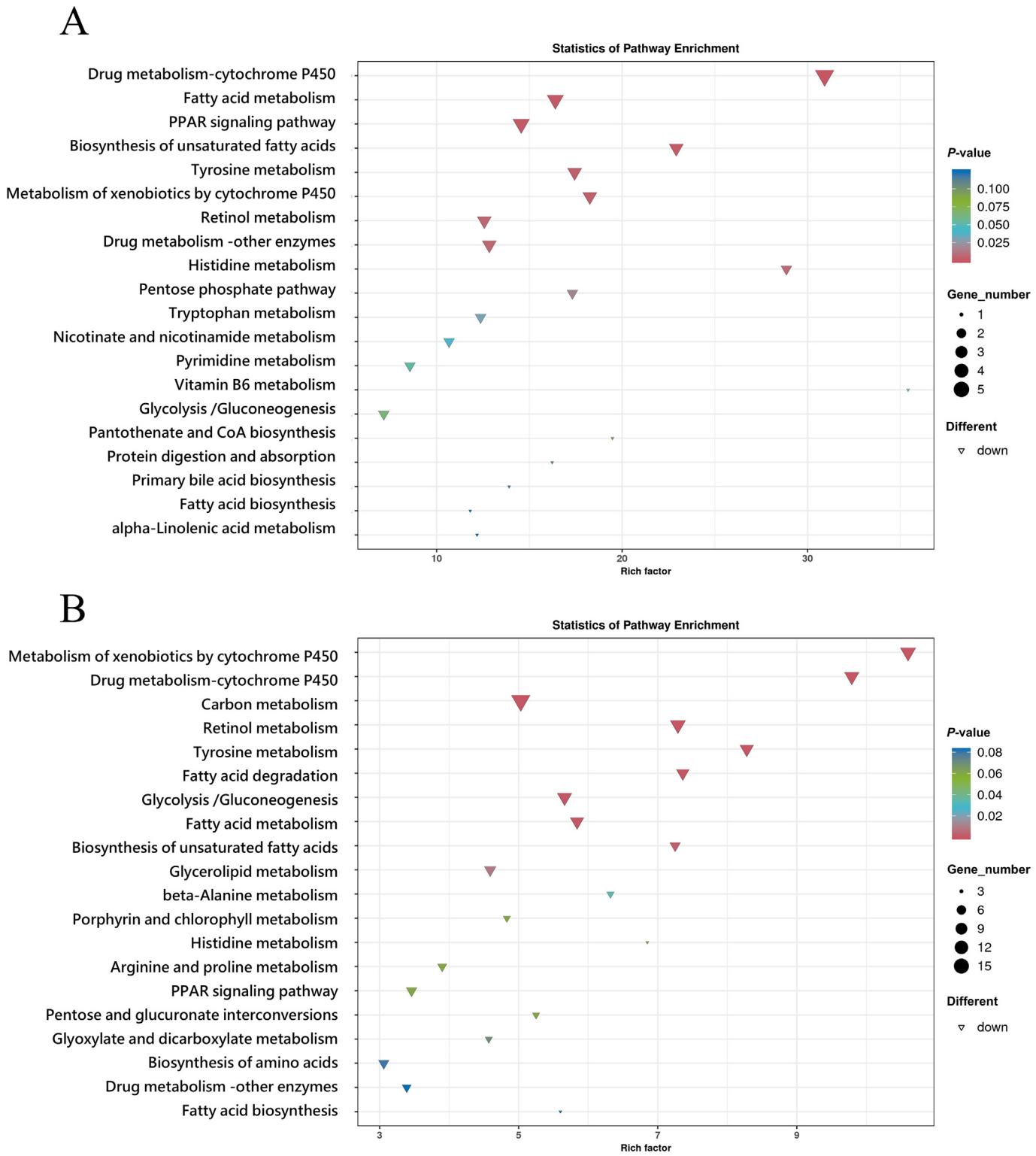

Fig. 12. KEGG bubble map (top 20) of down-regulated DEG in hybrid groupers fed diets with different aflatoxin B1 (AFB1) levels for 8 weeks. **(A)** Control vs AF445; **(B)** Control vs AF2230. Group control fed a basal diet, group AF445 fed a basal diet containing 445 μg/kg AFB1 and group AF2230 fed a basal diet containing 2230 μg/kg AFB1. DEG = differentially expressed genes; PPAR = peroxisome proliferator-activated receptor.

cyp450 enzymes, predominantly located in the liver's endoplasmic reticulum, are involved in both synthetic and catabolic processes and play a crucial role in cellular integrity, physiology, and defense (Guengerich, 2015). cyp450 has been shown to metabolize AFB1 in the liver (X. Wang et al., 2021). AFB1 is converted by cyp450 into electrophilic compounds, specifically AFBO, which can induce reactive oxygen species (ROS) production, leading to oxidative damage (Wu et al., 2020). Furthermore, AFBO can interact with intracellular macromolecules, causing damage to DNA, RNA, and proteins, and resulting in liver injury (Gallagher and

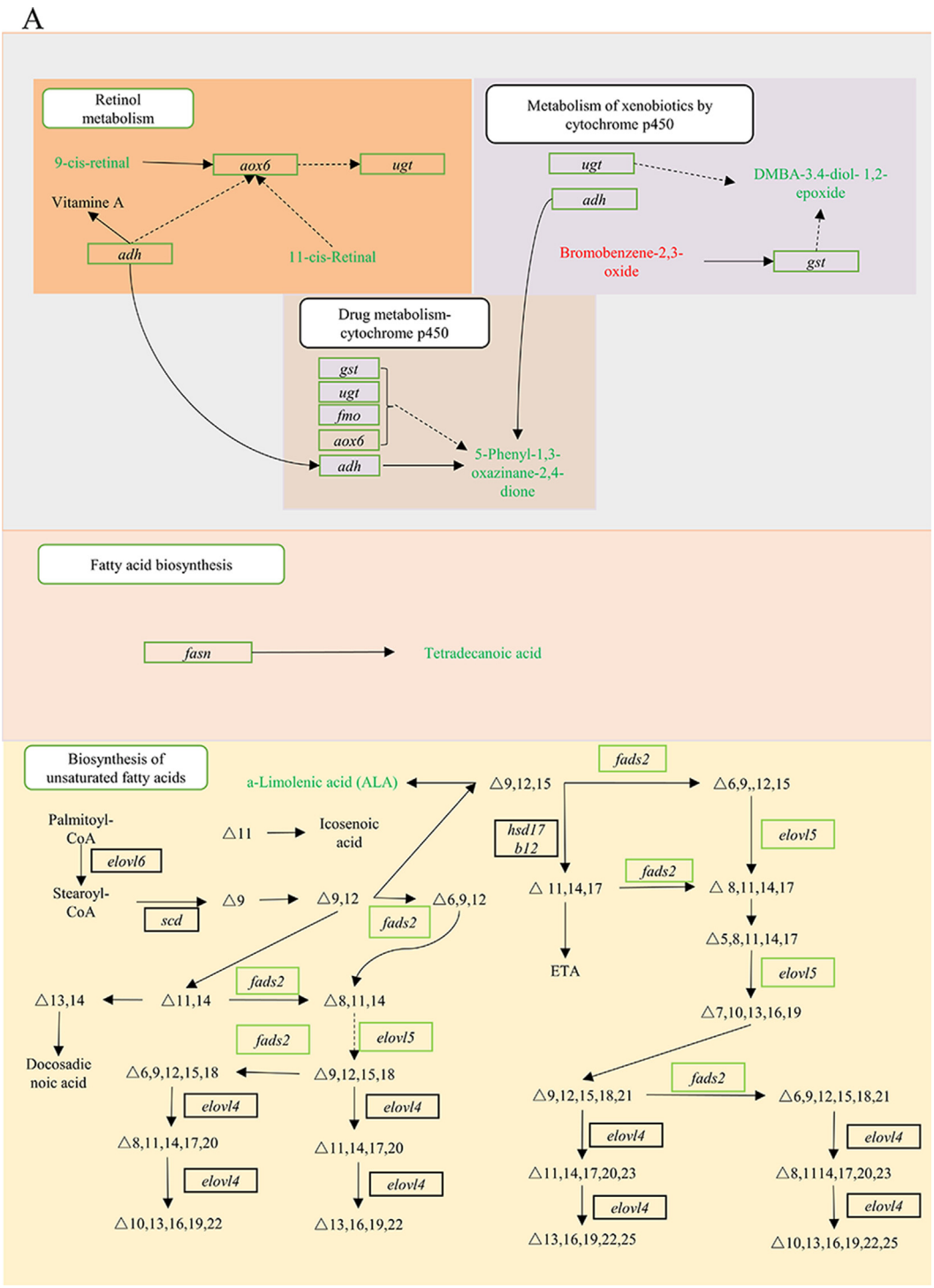

Fig. 13. Integrative analysis of metabolomics and transcriptomics. **(A)** Control vs AF445, **(B)** Control vs AF2230. Pathway overview of the unsynchronized growth of differentially expressed genes (DEG) and differential metabolites (DM) in significant pathways identified by multi-omics analysis. The DEG abbreviations are shown in either red boxes (highly expressed in the AF445 or AF2230 group) or green boxes (highly expressed in the control group). DM are shown either in red (highly expressed in the AF445 or AF2230 group) or green letters (highly expressed in the control group). Group control fed a basal diet, group AF445 fed a basal diet containing 445 μg/kg aflatoxin B1 (AFB1) and group AF2230 fed a basal diet containing 2230 μg/kg AFB1. *aox6* = aldehyde oxidase 6; *ugt* = glucuronosyltransferase; *adh* = alcohol dehydrogenase 1/7; *cyp3a* = cytochrome P450 family 3 subfamily A; *gst* = glutathione S-transferase; *fmo* = dimethylaniline monooxygenase; *dpys* = dihydropyrimidinase; *pgam* = 2,3-bisphosphoglycerate-dependent phosphoglycerate mutase; *agxt* = alanine-glyoxylate transaminase; *bhmt* = betaine-homocysteine S-methyltransferase; *alas2* = 5-aminolevulinate synthase; *spt* = serine palmitoyltransferase; *gal3st1* = galactosylceramide sulfotransferase; *cerk* = ceramide kinase; *retsat* = all-trans-retinol 13,14-reductase; *cyp26* = cytochrome P450 family 26; *dgat1* = diacylglycerol O-acyltransferase 1; *ggt1_5* = gamma-glutamyltranspeptidase; *cyp2j* = cytochrome P450 family 2 subfamily J; *pla2g* = secretory phospholipase A2; *fads2* = acyl-CoA 6-desaturase; 12-OPDA = (9S,13S,15Z)-12-Oxophyto-10,15-dienoate; *gabrg* = gamma-aminobutyric acid receptor subunit gamma; *acsl* = long-chain acyl-CoA synthetase; *acaa2* = acetyl-CoA acyltransferase 2; *elovl4* = elongation of very long chain fatty acids protein 4; *elovl5* = elongation of very long chain fatty acids protein 5; *elovl6* = elongation of very long chain fatty acids protein 6; *scd* = stearoyl-CoA desaturase; ETA = icosatrienoic acid; *fasn* = fatty acid synthase, animal type.

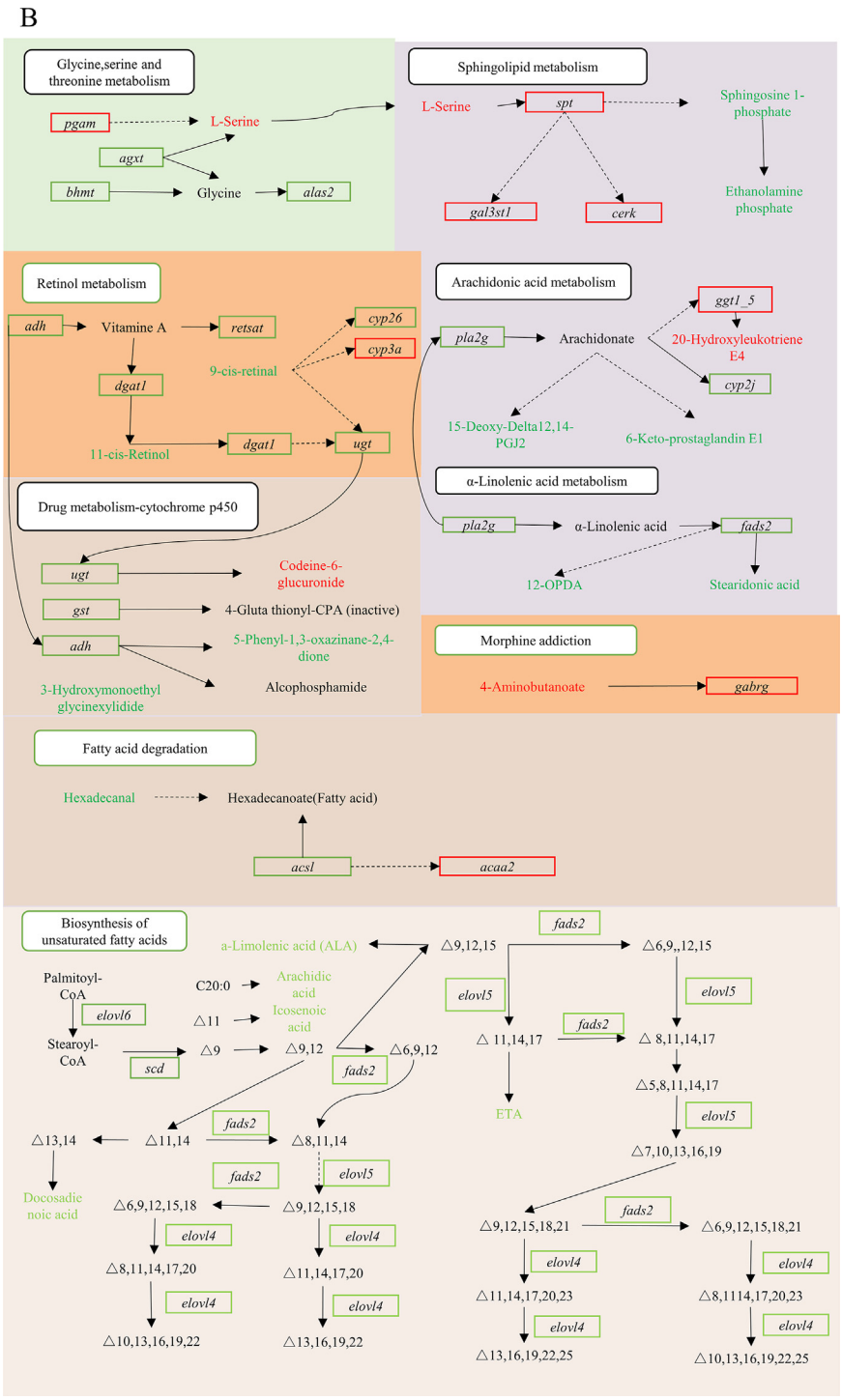

Fig. 13. (*continued*).

Eaton, 1995). In our experiment, differential gene and metabolite expression was observed in the pathways of "metabolism of xenobiotics by cytochrome P450" and "drug metabolism-cytochrome P450" across the AFB1-exposed groups and the control group. Specifically, the expression of cytochrome P450 family 2 subfamily J member 2 (*cyp2j2*) was downregulated in both exposed groups, while *cyp3a* was upregulated. The bioactivation of AFB1 by *cyp2j2* has not been previously reported. The upregulation of *cyp3a* in the exposed groups suggests its role in producing AFBO and ROS, potentially damaging the liver, as evidenced by H&E staining and ROS (Liu et al., 2023). However, there were differences; for instance, "drug metabolism-cytochrome P450" was downregulated in the AF445 group, while codeine-6-glucuronide levels were upregulated in the AF2230. Additionally, the expression of dimethylaniline monooxygenase (*fmo*) and aldehyde oxidase 6 (*aox6*) were not downregulated in the AF2230 group. Codeine-6-glucuronide is primarily produced through the action of glucuronosyltransferase (ugt2b7) on codeine (Eissing et al., 2012). fmo, a NADPH-dependent monooxygenase, catalyzes the oxidation of chemicals, drugs, and endogenous substrates containing nucleophilic nitrogen, sulfur,

and phosphorus atoms (McCarthy and Sinal, 2005). Aox are enzymes that metabolize aldehydes to carboxylic acids, abundant in the liver and involved in the metabolism of various exogenous chemicals, including drugs and toxins (Dalvie and Di, 2019). There is no direct evidence linking codeine-6-glucuronide with AFB1 metabolism, nor is there evidence that fmo and aox6 are directly involved in AFB1 metabolism or detoxification. The lack of downregulation of *fmo* and *aox* in the exposed group may relate to individual variability. Since the liver is the primary site for drug metabolism and detoxification, factors affecting liver function, such as the expression level of *fmo* and *aox6*, may indirectly influence AFB1 metabolism and detoxification. Further research is necessary to elucidate the specific roles and contributions of fmo and aox6 in AFB1 metabolism.

In addition to glutathione (gsh) binding, which is dependent on gst activity, uridine diphosphate − glucuronic acids (udpgt) binding is also crucial for the detoxification of AFB1, largely relying on ugt activity (Deng et al., 2020). Ugt represents a significant class of liver enzymes that conjugate drugs, toxins, and endogenous metabolites with glucuronic acid, thereby enhancing their water solubility and facilitating excretion (Du et al., 2018; Xu et al., 2020; Zhou et al., 2021). In this study, *ugt* expression levels were markedly lower in the AFB1-exposed groups (AF445 and AF2230) compared to the control group, indicating that the uridine diphosphate glucuronic acid (udpga)-binding metabolic pathway may be inhibited at higher AFB1 doses. An in vitro study has demonstrated that 100 μmol/L AFB1 and AFG1 exert a broad inhibitory effect on ugt isozymes, particularly ugt1a7 and ugt1a8 (Du and Liu, 2023). However, contrasting results were observed in human hepatocellular carcinoma cells (HepG2), where 10 μmol/L AFB1 significantly elevated the mRNA expression levels of *ugt1a3*, *ugt2b10*, *ugt2b15*, and *ugt2b17*, with minimal impact on the mRNA expression levels of transcriptional regulators (Du and Liu, 2023). These discrepancies may stem from two factors: first, the metabolic profile of human hepatocellular carcinoma cells differs from that of fish cells, and second, the controlled conditions of in vitro experiments may not replicate the complexity of in vivo metabolism, which is influenced by individual variability, age, gender, and other factors. Additionally, in a tilapia study, ugt activity increased after 7 days of exposure to 3.2 mg/kg AFB1 but subsequently decreased at higher doses, returning to its initial activity level (Deng et al., 2020). Although liver ugt activity was not assessed in this study, the observed differences are plausible, considering the sampling occurred after 56 days of feeding, reflecting subacute long-term effects rather than short-term exposure. Furthermore, high dietary AFB1 doses may induce liver damage and cell death, potentially impacting liver cell function, including *ugt* expression and activity.

In this experiment, a significant increase in L-serine content and the expression levels of serine palmitoyltransferase (*spt*), galactosylceramide sulfotransferase (*gal3st1*), and ceramide kinase (*cerk*) was observed in the sphingolipid metabolism of the AF2230 group. Conversely, the contents of sphingosine 1-phosphate (S1P) and ethanolamine phosphate (PEtN) were significantly decreased. As shown in Fig. 9, the increase in L-serine content was the primary cause for the upregulation of *spt*, and the expression levels of *gal3st1* and *cerk* were also indirectly influenced by the *spt* expression level. The decrease in S1P and PEtN in the AF2230 group may be attributed to the involvement of other metabolic networks. The DGE in sphingolipid metabolism observed in this experiment indirectly impacted the expression of these two metabolites in the liver, and another contributing factor could be starvation. There is evidence that ethanolamine phosphate phosphorylase (etnppl) irreversibly degrades PEtN into acetaldehyde, ammonium, and inorganic phosphate under conditions of starvation (Basu et al., 2023). In the AF2230 group, it was observed that this group may have stimulated one of the stomach's contractile functions due to the high AFB1 content in the diet. Consequently, a large amount of regurgitated diet was consistently found in the fiberglass bucket half an hour after apparent satiation (a phenomenon not observed in other experimental groups), and the groupers exhibited behavior indicative of hunger, actively seeking food. This suggests that a state of starvation may have contributed to the decrease in PEtN levels. Although no literature directly addresses the impact of starvation on S1P, studies in *Saccharomyces cerevisiae* indicate that AFB1 toxicity induces gluconeogenesis and inhibits sphingolipid metabolism, a response to toxins that is also observed in mammals (Suzuki and Iwahashi, 2009).

The overall disruption of liver lipid metabolism pathways in the hybrid grouper after exposure to AFB1 is substantial. One of the most striking findings in the current study was the downregulation of the biosynthesis of unsaturated fatty acids (Fig. 9). Compared to the control group, the gene expression levels of delta-6 desaturase (*fads2*) and elongation of very long chain fatty acids protein 5 (*elovl5*) showed significant downregulation in the AF445 group, and among the metabolites, α-linolenic acid (ALA) was also reduced. In the AF2230 group, in addition to the downregulation of *fads2* and *elovl5*, the expression levels of elongation of very long chain fatty acids protein 4 (*elovl4*), elongation of very long chain fatty acids protein 6 (*elovl6*), and delta-9 desaturase (*scd*) were downregulated, and metabolites such as ALA, arachidic acid, icosatrienoic acid (ETA), and docosadienoic acid showed significant decreases. This suggests that in the diet, AFB1 interferes with liver unsaturated fatty acid synthesis in the hybrid groupers, with more pronounced effects at higher doses. The lipid content of whole-body and muscle was significantly lower in the groupers exposed to a high dose of AFB1 compared to the control group, and a significant increase in the saturated fatty acid content along with a decrease in the unsaturated fatty acid content was observed in the muscle tissues of the AFB1-treated groupers. This is consistent with the trend observed in the present study for the biosynthesis of unsaturated fatty acids in the liver transcriptome, indicating that a high dose of AFB1 has a severe impact on the lipid metabolism of the groupers. Similar findings were reported in a rat study, where the liver of rats exposed to high doses of AFB1 exhibited defects in lipid metabolism (Galhardi et al., 2004; Lu et al., 2013). Previously published papers found that hepatic ROS levels were significantly higher in both the AF445 and AF2230 groups compared to the control group (Liu et al., 2023), suggesting that oxidative stress in the liver of groupers fed with 445 and 2230 μg/kg of AFB1 could lead to lipid metabolism disorders. It is also noteworthy that liver *fads2*, *elovl5*, and ALA were downregulated in both the AF445 and AF2230 groups. The *fads2* gene is responsible for converting polyunsaturated fatty acids, such as linolenic acid and α-linolenic acid, into longer-chained and more unsaturated forms like arachidonic acid (AA) and eicosapentaenoic acid (EPA) (Glaser et al., 2010). Although there may not be many specific studies on the direct interaction between *fads2* and AFB1, it is hypothesized that elevated liver ROS could influence *fads2* expression. A study on non-alcoholic fatty liver disease (NAFLD) found a significant decrease in fads2 activity in the liver in the presence of oxidative stress (Araya et al., 2010), and an increase in free radical activity in target tissues such as the liver (Videla et al., 2006, 2004), which may promote the direct inactivation of *fads2* and/or destabilization of the desaturase mRNA, leading to derangement of *fads2* expression. ALA and other omega-3 fatty acids are believed to have protective effects and the ability to mitigate cellular damage induced by oxidative stress. ALA is particularly susceptible to ROS-induced oxidative damage (Lin et al., 2021). Oxidative stress can lead to the peroxidation of ALA and other

polyunsaturated fatty acids (PUFA), forming lipid peroxides that can break down into various harmful secondary products, such as aldehydes and free radicals, which can damage cell membranes, proteins, and DNA. This is supported by the liver H&E results of the current study. The potential role of omega-3 fatty acids in protecting cells from ROS damage is further emphasized in an article discussing the anti-inflammatory and antioxidant stress effects of omega-3 long-chain polyunsaturated fatty acids in the treatment of retinal diseases (Jie et al., 2023). Therefore, it is plausible that the decrease in ALA observed in the current study was due to AFB1-induced oxidative stress in the liver.

In summary, retinol metabolism, metabolism of xenobiotics by cytochrome, drug metabolism-cytochrome P450, biosynthesis of unsaturated fatty acids, and oxidative stress were closely associated with AFB1-induced liver injury in hybrid groupers, as well as AFB1 metabolism in the liver.

5. Conclusion

In this research, the hepatotoxic mechanism of AFB1 in hybrid groupers was thoroughly examined through an integrated approach of transcriptomic and metabolomic analyses. The findings indicated that AFB1 exposure markedly elevated hepatic AFB1 levels in hybrid groupers, resulting in substantial histological liver damage and a concurrent significant increase in serum biochemical markers, such as ALT, AST, and LDH, indicative of hepatic dysfunction. The integrated analyses unveiled several metabolic pathways implicated in AFB1 metabolism, including retinol metabolism, xenobiotic metabolism via cytochrome P450, cytochrome P450 drug metabolism, unsaturated fatty acid biosynthesis, and sphingolipid metabolism, with observed variations in the activities of these pathways. This study suggests that AFB1 exposure induces liver injury and oxidative stress by perturbing hepatic metabolic pathways, offering novel insights into the toxicological effects of AFB1 on aquatic species and contributing to a scientific foundation for the health and sustainability of aquaculture practices.

Credit author contribution statement

Hao Liu: Writing-original draft preparation, Conceptualization, Methodology, Software. **Shuqing Liang:** Data curation. **Weibin Huang, and Yuanzhi Yang:** Methodology. **Menglong Zhou:** Validation, Investigation. **Baiquan Lu, Biao Li, and Wenshan Cai:** Supervision. **Hengyang Song, Beiping Tan, and Xiaohui Dong:** Conceptualization, Writing-Review and Editing, Project administration.

Declaration of competing interest

We declare that we have no financial and personal relationships with other people or organizations that can inappropriately influence our work, and there is no professional or other personal interest of any nature or kind in any product, service and/or company that could be construed as influencing the content of this paper.

Acknowledgments

This study was supported financially by the Research and Demonstration of Precision Functional Compound Feed Technology of Major Cultured Fishes and Shrimps in South China, China (2021B0202050002), the Department of Education of Guangdong Province, China (2021ZDZX4005), and the China Agriculture Research System of MOF and MARA, China (CARS-47).

Appendix A. Supplementary data

Supplementary data to this article can be found online at https://doi.org/10.1016/j.aninu.2024.08.002.

References

Abdelhiee EY, Elbialy ZI, Saad AH, Dawood MAO, Aboubakr M, El-Nagar SH, et al. The impact of *Moringa oleifera* on the health status of Nile tilapia exposed to aflatoxicosis. Aquaculture 2021;533:736110. https://doi.org/10.1016/j.aquaculture.2020.736110.

Ali Rajput S, Sun L, Zhang N, Mohamed Khalil M, Gao X, Ling Z, et al. Ameliorative effects of grape seed proanthocyanidin extract on growth performance, immune function, antioxidant capacity, biochemical constituents, liver histopathology and aflatoxin residues in broilers exposed to aflatoxin b1. Toxins 2017;9:371. https://doi.org/10.3390/toxins9110371.

Alpsoy L, Yalvac ME. Key roles of vitamins A, C, and E in aflatoxin B1-induced oxidative stress. In: Litwack G, editor. Vitam. Horm.. 1st ed.vol. 86; 2011. p. 287–305. https://doi.org/10.1016/B978-0-12-386960-9.00012-5. Istanbul.

AOAC. Official methods of analysis. 18th ed. Gaithersburg, MD, USA: AOAC International; 2006.

Araya J, Rodrigo R, Pettinelli P, Araya AV, Poniachik J, Videla LA. Decreased liver fatty acid Δ-6 and Δ-5 desaturase activity in obese patients. Obesity 2010;18:1460–3. https://doi.org/10.1038/oby.2009.379.

Ayyat MS, Ayyat AMN, Al-Sagheer AA, El-Hais AEAM. Effect of some safe feed additives on growth performance, blood biochemistry, and bioaccumulation of aflatoxin residues of Nile tilapia fed aflatoxin-B1 contaminated diet. Aquaculture 2018;495:27–34. https://doi.org/10.1016/j.aquaculture.2018.05.030.

Barany A, Guilloto M, Cosano J, de Boevre M, Oliva M, de Saeger S, et al. Dietary aflatoxin B1 (AFB1) reduces growth performance, impacting growth axis, metabolism, and tissue integrity in juvenile gilthead sea bream (*Sparus aurata*). Aquaculture 2021;533:736189. https://doi.org/10.1016/j.aquaculture.2020.736189.

Basu S, Pawlowic MC, Hsu FF, Thomas G, Zhang K. Ethanolaminephosphate cytidylyltransferase is essential for survival, lipid homeostasis and stress tolerance in *Leishmania major*. PLoS Pathog 2023;19:1–28. https://doi.org/10.1371/journal.ppat.1011112.

Blaner WS, Li Y, Brun PJ, Yuen JJ, Lee SA, Clugston RD. Vitamin A absorption, storage and mobilization. In: Asson-Batres MA, Rochette-Egly C, editors. Subcell. Biochem.. 1st ed.vol. 81. Dordrecht: Springer; 2016. p. 95–125. https://doi.org/10.1007/978-94-024-0945-1_4.

Blomhoff R, Blomhoff HK. Overview of retinoid metabolism and function. J Neurobiol 2006;66:606–30. https://doi.org/10.1002/neu.20242.

Bu H, Li Y. Pathology. 9th ed. Beijing: People's Medical Publishing House; 2018.

Bureau of Fisheries of the Ministry of Agriculture and Rural Affairs (MARA) of the People's Republic of China. China Fishery statistical yearbook. Beijing, China: China Agriculture Press; 2020. p. 24–34.

Cassand P, Decoudu S, Lévêque F, Daubèze M, François Narbonne J. Effect of vitamin E dietary intake on in vitro activation of aflatoxin B1. Mutat Res Toxicol 1993;319:309–16. https://doi.org/10.1016/0165-1218(93)90020-E.

Ch'ng CL, Senoo S. Egg and lar val development of a new hybrid grouper, tiger grouper *Epinephelus fuscoguttatus* giant grouper *E. lanceolatus*. Aquac Sci 2008;56:505–12. https://doi.org/10.11233/aquaculturesci.56.505.

Dalvie D, Di L. Aldehyde oxidase and its role as a drug metabolizing enzyme. Pharmacol Ther 2019;201:137–80. https://doi.org/10.1016/j.pharmthera.2019.05.011.

Deng S, Tian L, Liu F, Jin S, Liang G, Yang H, et al. Toxic effects and residue of aflatoxin B1 in tilapia (*Oreochromis niloticus* × *O. aureus*) during long-term dietary exposure. Aquaculture 2010;307:233–40. https://doi.org/10.1016/j.aquaculture.2010.07.029.

Deng Y, Deng Q, Wang Y, Sun L, Wang R, Ye L, et al. Tolerance and bio-accumulation of aflatoxin B1 in invertebrate *Litopenaeus vannamei* and vertebrate *Oreochromis niloticus*. Aquaculture 2020;524:735055. https://doi.org/10.1016/j.aquaculture.2020.735055.

Dohnal V, Wu Q, Kuča K. Metabolism of aflatoxins: key enzymes and interindividual as well as interspecies differences. Arch Toxicol 2014;88:1635–44. https://doi.org/10.1007/s00204-014-1312-9.

Du H, Xiong S, Lv H, Zhao S, Manyande A. Comprehensive analysis of transcriptomics and metabolomics to understand the flesh quality regulation of crucian carp (*Carassius auratus*) treated with short term micro-flowing water system. Food Res Int 2021;147:110519. https://doi.org/10.1016/j.foodres.2021.110519.

Du Z, Cao Y, Li S, Hu C, Fu Z, Huang C, et al. Inhibition of UDP-glucuronosyltransferases (UGTs) by phthalate monoesters. Chemosphere 2018;197:7–13. https://doi.org/10.1016/j.chemosphere.2018.01.010.

Du Z, Liu Z. Inhibition of aflatoxins on UDP-glucuronosyltransferases (UGTs). Toxicol Vitr 2023;90:105612. https://doi.org/10.1016/j.tiv.2023.105612.

Eissing T, Lippert J, Willmann S. Pharmacogenomics of codeine, morphine, and morphine-6-glucuronide. Mol Diagn Ther 2012;16:43–53. https://doi.org/10.1007/BF03256429.

El-Sayed YS, Khalil RH. Toxicity, biochemical effects and residue of aflatoxin B1 in marine water-reared sea bass (*Dicentrarchus labrax* L.). Food Chem Toxicol 2009;47:1606–9. https://doi.org/10.1016/j.fct.2009.04.008.

Eshelli M, Qader MM, Jambi EJ, Hursthouse AS, Rateb ME. Current status and future opportunities of omics tools in mycotoxin research. Toxins 2018;10:1–26. https://doi.org/10.3390/toxins10110433.
Farabi SMV, Yousefian M, Hajimoradloo A. Aflatoxicosis in juvenile *Huso huso* fed a contaminated diet. J Appl Ichthyol 2006;22:234–7.
Galhardi CM, Diniz YS, Faine LA, Rodrigues HG, Burneiko RCM, Ribas BO, et al. Toxicity of copper intake: lipid profile, oxidative stress and susceptibility to renal dysfunction. Food Chem Toxicol 2004;42:2053–60. https://doi.org/10.1016/j.fct.2004.07.020.
Gallagher EP, Eaton DL. In vitro biotransformation of aflatoxin B1 (AFB1) in channel catfish liver. Toxicol Appl Pharmacol 1995;132:82–90. https://doi.org/10.1006/taap.1995.1089.
Ghadiri S, Spalenza V, Dellafiora L, Badino P, Barbarossa A, Dall'Asta C, et al. Modulation of aflatoxin B1 cytotoxicity and aflatoxin M1 synthesis by natural antioxidants in a bovine mammary epithelial cell line. Toxicol Vitr 2019;57:174–83. https://doi.org/10.1016/j.tiv.2019.03.002.
Ghyselinck NB, Båvik C, Sapin V, Mark M, Bonnier D, Hindelang C, et al. Cellular retinol-binding protein I is essential for vitamin A homeostasis. EMBO J 1999;18:4903–14. https://doi.org/10.1093/emboj/18.18.4903.
Glaser C, Heinrich J, Koletzko B. Role of FADS1 and FADS2 polymorphisms in polyunsaturated fatty acid metabolism. Metabolism 2010;59:993–9. https://doi.org/10.1016/j.metabol.2009.10.022.
Grabherr MG, Haas BJ, Yassour M, Levin JZ, Thompson DA, Amit I, et al. Full-length transcriptome assembly from RNA-Seq data without a reference genome. Nat Biotechnol 2011;29:644–52. https://doi.org/10.1038/nbt.1883.
Guengerich FP. Human cytochrome P450 enzymes. In: Cytochrome P450. Cham: Springer International Publishing; 2015. p. 523–785. https://doi.org/10.1007/978-3-319-12108-6_9.
Hanioka N, Nonaka Y, Saito K, Negishi T, Okamoto K, Kataoka H, et al. Effect of aflatoxin B1 on UDP-glucuronosyltransferase mRNA expression in HepG2 cells. Chemosphere 2012;89:526–9. https://doi.org/10.1016/j.chemosphere.2012.05.039.
Huang Y, Han D, Zhu X, Yang Y, Jin J, Chen Y, et al. Response and recovery of gibel carp from subchronic oral administration of aflatoxin B1. Aquaculture 2011;319:89–97. https://doi.org/10.1016/j.aquaculture.2011.06.024.
Iyanagi T, Xia C, Kim JJP. NADPH-cytochrome P450 oxidoreductase: prototypic member of the diflavin reductase family. Arch Biochem Biophys 2012;528:72–89. https://doi.org/10.1016/j.abb.2012.09.002.
Jie W, Guoge H, Quanhong H. Macular mechanism and research status of ω-3 long-chain polyunsaturated fatty acids in the treatment of retinal diseases. Chin J Optom Ophthalmol Vis Sci 2023;25:715–20. https://doi.org/10.3760/cma.j.cn115909-20220125-00041.
Kono M, Goletz PW, Crouch RK. 11-cis- and all-trans-retinols can activate rod opsin: rational design of the visual cycle. Biochemistry 2008;47:7567–71. https://doi.org/10.1021/bi800357b.
Kuilman MEM, Maas RFM, Fink-Gremmels J. Cytochrome P450-mediated metabolism and cytotoxicity of aflatoxin B1 in bovine hepatocytes. Toxicol Vitr 2000;14:321–7. https://doi.org/10.1016/S0887-2333(00)00025-4.
Kuilman MEM, Maas RFM, Judah DJ, Fink-Gremmels J. Bovine hepatic metabolism of aflatoxin B1. J Agric Food Chem 1998;46:2707–13. https://doi.org/10.1021/jf980062x.
Lin W, Shen P, Song Y, Huang Y, Tu S. Reactive oxygen species in autoimmune cells: function, differentiation, and metabolism. Front Immunol 2021;12:1–16. https://doi.org/10.3389/fimmu.2021.635021.
Liu H, Dong X, Tan B, Du T, Zhang S, Yang Y, et al. Effects of two dietary protein levels on growth, body composition, intestinal microflora and expression of TOR, IGF-I, LPL and HSP70 of juvenile silver sillago, *Sillago sihama*. Aquac Nutr 2021;533:1–13. https://doi.org/10.1111/anu.13357.
Liu H, Xie R, Huang W, Yang Y, Zhou M, Lu B, et al. Negative effects of aflatoxin B1 (AFB1) in the diet on growth performance, protein and lipid metabolism, and liver health of juvenile hybrid grouper (*Epinephelus fuscoguttatus*♀ × *Epinephelus lanceolatus*♂). Aquac Rep 2023;33:101779. https://doi.org/10.1016/j.aqrep.2023.101779.
Liu H, Yang J-J, Dong X-H, Tan B, Zhang S, Chi S, et al. Effects of different dietary carbohydrate-to-lipid ratios on growth, plasma biochemical indexes, digestive, and immune enzymes activities of sub-adult orange-spotted grouper *Epinephelus coioides*. Fish Physiol Biochem 2020;46:1409–20. https://doi.org/10.1007/s10695-020-00799-4.
Livak KJ, Schmittgen TD. Analysis of relative gene expression data using real-time quantitative PCR and the $2^{-\Delta\Delta CT}$ method. Methods 2001;25:402–8. https://doi.org/10.1006/meth.2001.1262.
Lu X, Hu B, Shao L, Tian Y, Jin T, Jin Y, et al. Integrated analysis of transcriptomics and metabonomics profiles in aflatoxin B1-induced hepatotoxicity in rat. Food Chem Toxicol 2013;55:444–55. https://doi.org/10.1016/j.fct.2013.01.020.
Mao X, Cai T, Olyarchuk JG, Wei L. Automated genome annotation and pathway identification using the KEGG Orthology (KO) as a controlled vocabulary. Bioinformatics 2005;21:3787–93. https://doi.org/10.1093/bioinformatics/bti430.
Martins DA, Engrola S, Morais S, Bandarra N, Coutinho J, Yúfera M, et al. Cortisol response to air exposure in *Solea senegalensis* post-larvae is affected by dietary arachidonic acid-to-eicosapentaenoic acid ratio. Fish Physiol Biochem 2011;37:733–43. https://doi.org/10.1007/s10695-011-9473-4.
Masia R, McCarty WJ, Lahmann C, Luther J, Chung RT, Yarmush ML, et al. Live cell imaging of cytosolic NADH/NAD^+ ratio in hepatocytes and liver slices. Am J Physiol Liver Physiol 2018;314:G97–108. https://doi.org/10.1152/ajpgi.00093.2017.
McCarthy TC, Sinal CJ. Biotransformation. In: Wexler PBT, editor. Encycl. Toxicol. 2nd ed. New York: Elsevier; 2005. p. 299–312. https://doi.org/10.1016/B0-12-369400-0/00137-X.
McLean M, Dutton MF. Cellular interactions and metabolism of aflatoxin: an update. Pharmacol Ther 1995;65:163–92. https://doi.org/10.1016/0163-7258(94)00054-7.
Mwihia E, Mbuthia P, Eriksen G, Gathumbi J, Maina J, Mutoloki S, et al. Occurrence and levels of aflatoxins in fish feeds and their potential effects on fish in Nyeri, Kenya. Toxins 2018;10:543. https://doi.org/10.3390/toxins10120543.
Nayak S, Sashidhar RB. Metabolic intervention of aflatoxin B1 toxicity by curcumin. J Ethnopharmacol 2010;127:641–4. https://doi.org/10.1016/j.jep.2009.12.010.
Ottinger CA, Kaattari SL. Sensitivity of rainbow trout leucocytes to aflatoxin B1. Fish Shellfish Immunol 1998;8:515–30. https://doi.org/10.1006/fsim.1998.0154.
Pauletto M, Tolosi R, Giantin M, Guerra G, Barbarossa A, Zaghini A, et al. Insights into aflatoxin B1 toxicity in cattle: an in vitro whole-transcriptomic approach. Toxins 2020;12:1–28. https://doi.org/10.3390/toxins12070429.
Percie du Sert N, Hurst V, Ahluwalia A, Alam S, Avey MT, Baker M, et al. The ARRIVE guidelines 2.0: updated guidelines for reporting animal research. J Cereb Blood Flow Metab 2020;40:1769–77. https://doi.org/10.1177/0271678X20943823.
Pérez-Acosta JA, Burgos-Hernandez A, Velázquez-Contreras CA, Márquez-Ríos E, Torres-Arreola W, Arvizu-Flores AA, et al. An in vitro study of alkaline phosphatase sensitivity to mixture of aflatoxin B1 and fumonisin B1 in the hepatopancreas of coastal lagoon wild and farmed shrimp *Litopenaeus vannamei*. Mycotoxin Res 2016;32:117–25. https://doi.org/10.1007/s12550-016-0246-x.
Royes J, Yanong R. Molds in fish feeds and aflatoxicosis 1. Univ Florida Ext; 2010. p. 1–4.
Rushing BR, Selim MI. Aflatoxin B1: a review on metabolism, toxicity, occurrence in food, occupational exposure, and detoxification methods. Food Chem Toxicol 2019;124:81–100. https://doi.org/10.1016/j.fct.2018.11.047.
Saba N, Seal A. Comparative study of binding pockets in human CYP1A2, CYP3A4, CYP3A5, and CYP3A7 with aflatoxin B1, a hepato-carcinogen, by molecular dynamics simulation & principal component analysis. Curr Drug Metab 2022;23:521–37. https://doi.org/10.2174/1389200223666220718161754.
Santangeli S, Notarstefano V, Maradonna F, Giorgini E, Gioacchini G, Forner-Piquer I, et al. Effects of diethylene glycol dibenzoate and Bisphenol A on the lipid metabolism of *Danio rerio*. Sci Total Environ 2018;636:641–55. https://doi.org/10.1016/j.scitotenv.2018.04.291.
Suzuki KT. Metabolomics of arsenic based on speciation studies. Anal Chim Acta 2005;540:71–6. https://doi.org/10.1016/j.aca.2004.09.092.
Suzuki T, Iwahashi Y. Gene expression profile of MAP kinase PTC1 mutant exposed to aflatoxin B1: dysfunctions of gene expression in glucose utilization and sphingolipid metabolism. Chem Bio Inform J 2009;9:94–107. https://doi.org/10.1273/cbij.9.94.
Tang L, Xu L, Afriyie-Gyawu E, Liu W, Wang P, Tang Y, et al. Aflatoxin–albumin adducts and correlation with decreased serum levels of vitamins A and E in an adult Ghanaian population. Food Addit Contam A 2009;26:108–18. https://doi.org/10.1080/02652030802308472.
Tu H, Peng X, Yao X, Tang Q, Xia Z, Li J, et al. Integrated transcriptomic and metabolomic analyses reveal low-temperature tolerance mechanism in giant freshwater prawn *Macrobrachium rosenbergii*. Animals 2023;13:1605. https://doi.org/10.3390/ani13101605.
Videla LA, Rodrigo R, Araya J, Poniachik J. Insulin resistance and oxidative stress interdependency in non-alcoholic fatty liver disease. Trends Mol Med 2006;12:555–8. https://doi.org/10.1016/j.molmed.2006.10.001.
Videla LA, Rodrigo R, Orellana M, Fernandez V, Tapia G, Quiñones L, et al. Oxidative stress-related parameters in the liver of non-alcoholic fatty liver disease patients. Clin Sci 2004;106:261–8. https://doi.org/10.1042/CS20030285.
Wang C, Li A, Wang W, Cong R, Wang L, Zhang G, et al. Integrated application of transcriptomics and metabolomics reveals the energy allocation-mediated mechanisms of growth-defense trade-offs in *Crassostrea gigas* and *Crassostrea angulata*. Front Mar Sci 2021;8:1–16. https://doi.org/10.3389/fmars.2021.744626.
Wang X, He Y, Tian J, Muhammad I, Liu M, Wu C, et al. Ferulic acid prevents aflatoxin B1-induced liver injury in rats via inhibiting cytochrome P450 enzyme, activating Nrf2/GST pathway and regulating mitochondrial pathway. Ecotoxicol Environ Saf 2021;224:112624. https://doi.org/10.1016/j.ecoenv.2021.112624.
Wang X, Wang Y, Wang R, Lyu P. Mycotoxins contamination situation and toxicity evaluation of moldy aquatic feed in southern Guangdong of China. Acta Agric Zhejiangensis 2016;28:951–8.
Wogan GN, Kensler TW, Groopman JD. Present and future directions of translational research on aflatoxin and hepatocellular carcinoma. A review. Food Addit Contam A 2012;29:249–57. https://doi.org/10.1080/19440049.2011.563370.
Wu H, Wang Q, Yang H, Ahsan H, Tsai W, Wang L, et al. Aflatoxin B1 exposure, hepatitis b virus infection, and hepatocellular carcinoma in Taiwan. Cancer Epidemiol Biomark Prev 2009;18:846–53. https://doi.org/10.1158/1055-9965.EPI-08-0697.
Wu J, Gan Z, Zhuo R, Zhang L, Wang T, Zhong X. Resveratrol attenuates aflatoxin B1-Induced ROS formation and increase of m6A RNA methylation. Animals 2020;10:677. https://doi.org/10.3390/ani10040677.
Xu L, Zheng R, Xie P, Guo Q, Ji H, Li T. Dysregulation of UDP-glucuronosyltransferases in CCl4 induced liver injury rats. Chem Biol Interact 2020;325:109115. https://doi.org/10.1016/j.cbi.2020.109115.
Xu X, Yang H, Xu Z, Li X, Leng X. The comparison of largemouth bass (*Micropterus salmoides*) fed trash fish and formula feeds: growth, flesh quality and

metabolomics. Front Nutr 2022;9:1–14. https://doi.org/10.3389/fnut.2022.966248.
Yokoyama Y, Sasaki Y, Terasaki N, Kawataki T, Takekawa K, Iwase Y, et al. Comparison of drug metabolism and its related hepatotoxic effects in HepaRG, cryopreserved human hepatocytes, and HepG2 cell cultures. Biol Pharm Bull 2018;41:722–32. https://doi.org/10.1248/bpb.b17-00913.
Yu M, Zhang Y, Blaner WS, Santella RM. Influence of vitamins A, C, and E and β-carotene on aflatoxin B1 binding to DNA in woodchuck hepatocytes. Cancer 1994;73:596–604. https://doi.org/10.1002/1097-0142(19940201)73:3<596::AID-CNCR2820730316>3.0.CO;2-N.
Zhang X, Xiao J, Guo Z, Zhong H, Luo Y, Wang J, et al. Transcriptomics integrated with metabolomics reveals the effect of *Lycium barbarum* polysaccharide on apoptosis in Nile tilapia (*Oreochromis niloticus*). Genomics 2022;114:229–40. https://doi.org/10.1016/j.ygeno.2021.12.009.
Zhou Q, Qin W, Finel M, He Q, Tu D, Wang C, et al. A broad-spectrum substrate for the human UDP-glucuronosyltransferases and its use for investigating glucuronidation inhibitors. Int J Biol Macromol 2021;180:252–61. https://doi.org/10.1016/j.ijbiomac.2021.03.073.
Zhu X, Hao R, Tian C, Zhang J, Zhu C, Li G. Integrative transcriptomics and metabolomics analysis of body color formation in the leopard coral grouper (*Plectropomus leopardus*). Front Mar Sci 2021;8:1–13. https://doi.org/10.3389/fmars.2021.726102.
Zuckerman AJ. IARC monographs on the evaluation of carcinogenic risks to humans. J Clin Pathol 1995;48. https://doi.org/10.1136/jcp.48.7.691-a. 691–691.
Zychowski KE, Rodrigues Hoffmann A, Ly HJ, Pohlenz C, Buentello A, Romoser A, et al. The effect of aflatoxin-B1 on red drum (*Sciaenops ocellatus*) and assessment of dietary supplementation of NovaSil for the prevention of aflatoxicosis. Toxins 2013;5:1555–73. https://doi.org/10.3390/toxins5091555.